Atmospheric Research 340 (2026) 109071

Contents lists available at ScienceDirect

Atmospheric Research

journal homepage: www.elsevier.com/locate/atmosres

Levante and Poniente winds in the Strait of Gibraltar: Present and future characterization using regional climate models

María Ortega [a,b,c,*], Claudia Gutiérrez [d], Noelia López-Franca [c], María Ofelia Molina [e], William Cabos [d], Dmitry Sein [f,g], Enrique Sánchez [h]

[a] Climate Evaluation and Modelling Division, State Meteorological Agency (AEMET), Madrid, Spain
[b] Tragsatec, Tragsa Group, Madrid, Spain
[c] Environmental Sciences Institute, University of Castilla-La Mancha (UCLM), Toledo, Spain
[d] Department of Physics and Mathematics, University of Alcalá (UAH), Alcalá de Hernares, Spain
[e] Faculdade de Ciências, Universidade de Lisboa, Lisboa, Portugal
[f] Alfred Wegener Institute for Polar and Marine Research (AWI), Bremerhaven, Germany
[g] Moscow Institute of Physics and Technology, Moscow, Russia
[h] Faculty of Environmental Sciences and Biochemistry, University of Castilla-La Mancha (UCLM), Toledo, Spain

ARTICLE INFO

Dataset link: https://reanalysis.meteo.uni-bonn.de/?COSMO-REA6, https://cds.climate.copernicus.eu/cdsapp#!/dataset/reanalysis-era5-single-levels, https://www.euro-cordex.net/060378/index.php.en, https://www.medcordex.eu/medcordex.php

Keywords:
Levante
Poniente
Regional winds
Regional climate models
EURO-CORDEX
Med-CORDEX

ABSTRACT

Levante and Poniente are regional winds that appear in the Strait of Gibraltar with great intensity and frequency. However, they have not been the focus of many modelling studies so far. For this reason, the present work has two aims. First, to evaluate the capability to describe both winds using the largest available set of outputs from regional climate models and different wind data frequencies, spatial resolutions and atmosphere-ocean coupling characteristics. Second, to study wind changes between present (1950–2005) and future climate conditions (RCP8.5, 2006-2099). Results indicate that available spatial resolution is essential for a proper wind description. Internal physics are also a source of variation. Coupling effect does not lead to important changes on any of the studied regional winds. Levante occurs in the historical period between 110–130 days per year, covering 42%–44% of the Strait, with future increase of 10–20 annual events, depending on the model. Levante spatial extension varies with mixed trend signs. Poniente is detected between 135–155 days per year over 45%–50% of the Strait for the historical period and shows future debilitation in its magnitude with around 5–20 less days. This pioneering work manifests the capability of regional climate models to quantify Levante and Poniente events. Future climate change projections should be further studied to obtain as much regional climate model outputs as possible and to increase the robustness of such projections. Besides, a deeper analysis of weather variability patterns related to these wind conditions would strongly increase our understanding of the atmospheric mechanisms behind such important regional winds.

1. Introduction

Regional winds are defined as flows generated by small-scale processes. They extend up to hundreds of kilometres or less and last from seconds to days (Ahrens and Henson, 2019; Ortega et al., 2023, 2024). The Iberian Peninsula displays a complex orography and terrain, which gives rise to several regional winds (García de Pedraza, 1971; Tout and Kemp, 1985; Campins et al., 1995; Lorente-Plazas et al., 2015). Among the peninsular flows, Levante and Poniente, which appear along the entire coast, but with particular intensity in the Strait of Gibraltar and the southern peninsular area, stand out (Tout and Kemp, 1985; Martín García et al., 1989; García de Pedraza, 1990; García de Pedraza and García Vega, 2001; Ortega et al., 2023). Levante is an easterly wind characterized by cold conditions on the eastern coast and warm and dry weather on the western one (Tout and Kemp, 1985; García de Pedraza, 1990; Lorente-Plazas et al., 2015; Hidalgo and Gallego, 2019). Poniente is a westerly wind associated with rainy conditions on the western coast, but it is not as hot and dry as the eastern one (Tout and Kemp, 1985; Martín García et al., 1989; Viedma Muñoz, 2012). Ortega et al. (2023) concluded that each wind (defined for speeds larger than 5 m/s flowing from its corresponding direction) appears around 30% of days/year.

Levante usually appears due to European Blocking and Atlantic Ridge situations, among others (Ortega et al., 2023). For this wind to appear, there must be pressure differences between the Azores High

* Corresponding author at: Environmental Sciences Institute, University of Castilla-La Mancha (UCLM), Toledo, Spain.
E-mail address: morteg22@tragsa.es (M. Ortega).

https://doi.org/10.1016/j.atmosres.2026.109071
Received 12 February 2026; Received in revised form 5 May 2026; Accepted 6 May 2026
Available online 12 May 2026

extending over Europe and a low in North Africa (García de Pedraza, 1990; Lorente-Plazas et al., 2015; Hidalgo and Gallego, 2019). Furthermore, during NAO+ (North Atlantic Oscillation), which promotes an European Blocking configuration, the wind blows from the east, generating Levante situations (Jerez et al., 2013). Poniente appears under low-pressure conditions moving from the Atlantic and high-pressure ones in Africa (García de Pedraza, 1990; Hidalgo and Gallego, 2019; Ortega et al., 2023).

The study of these flows and the dynamics and mechanisms that drive them is of great importance to the inhabitants of the areas where they appear. Levante and Poniente winds modulate the climate and weather in these places, potentially leading to adverse conditions, so research into their future changes is also necessary (Tout and Kemp, 1985; Martín García et al., 1989; García de Pedraza, 1990; García de Pedraza and García Vega, 2001). The lack of characterization and research into their potential changes is a significant gap in the current climate landscape.

Studies of several European regional winds using climate models can be found in the literature (Small et al., 2012; Anagnostopoulou et al., 2014; Dafka et al., 2018a,b; Josipović et al., 2018; Obermann et al., 2018; Obermann-Hellhund et al., 2018; Obermann-Hellhund and Ahrens, 2018; Ezber, 2019; Belušić Vozila et al., 2019; Denamiel et al., 2020, 2021). Global climate models (GCMs) have, due to their resolution, limitations in describing these phenomena. Thus, the CORDEX (Coordinated Regional Climate Downscaling Experiment) initiative, based on regional climate models (RCMs) driven by GCMs over a specific area (Giorgi and Gutowski, 2015; Giorgi, 2019), could largely help to improve such resolution shortcomings. EURO-CORDEX (Jacob et al., 2020) and Med-CORDEX (Somot and Ruti, 2012; Ruti et al., 2016) initiatives offer a wealth of free-download models (https://www.euro-cordex.net/index.php.en, https://www.medcordex.eu/). Recent works based on high-resolution reanalyses (Ortega et al., 2023, 2024) conclude that COSMO-REA6 (Bollmeyer et al., 2015) can be sufficient to describe Levante and Poniente. In addition, to date there have been no works that study these winds using RCM ensembles which indicates that this work goes beyond the current state of the art in Iberian regional wind research.

The main objective of this work is to evaluate the capacity of regional climate models (REMO, MPIOM-REMO, ALADIN63, CNRM-RCSM4, RegCM4-6) to describe Levante and Poniente at the Strait of Gibraltar in the present climate as well as the future trends in these winds. First, a definition of Levante and Poniente, based on the methodology of Ortega et al. (2023) and Ortega et al. (2024), is used. The effect of temporal model resolution, as well as atmosphere-ocean coupling characteristics, is investigated. This analysis is carried out in the common evaluation period for all simulations (1995–2011), comparing them with two reanalysis (ERA5, COSMO-REA6). Changes are obtained comparing model historical period (1950–2005) with RCP8.5 scenario (2006–2099). Their main characteristics, extension size, hours of appearance and detected events are examined in both periods.

This paper is structured as follows. Data, regional wind definitions and methods are described in Section 2, and the results are presented in Section 3. These are discussed in Section 4 and main conclusions are detailed in Section 5.

2. Data and methods

2.1. Regional climate models

In this work, available RCMs forced by CMIP5 GCMs, mainly from the EURO-CORDEX (Gobiet et al., 2012; Jacob et al., 2012; Casanueva et al., 2016) and Med-CORDEX (Somot and Ruti, 2012; Ruti et al., 2016) projects, were downloaded. Models that did not have hourly or 3-hourly data were discarded, and all models available at the time of the study on the servers or under personal request were selected. The largest available range of different spatial resolutions and atmosphere-ocean coupling properties have been chosen to evaluate their impact on wind description. Used models are described below and can be consulted in Table 1.

Table 1
Models and reanalysis ("Reanal.") used for this work and their main characteristics. The common evaluation period for all of them was 1995–2011. For the models, both historical (1950–2005) and RCP8.5 emissions scenario (2006–2099) were used. DR = driving reanalysis. SR = spatial resolution (degrees). TR = temporal resolution (h). C = coupling.

Name	Type	Institute	DR	SR	TR	C
ERA5	Reanal.	ECMWF		0.25°	1	
COSMO-REA6	Reanal.	DWD		0.055	1	
REMO	Model	Max Planck	Era-Interim	0.22°	3	No
MPIOM-REMO	Model	Max Planck	Era-Interim	0.22°	3	Yes
ALADIN63 (3h)	Model	CNRM	Era-Interim	0.11°	3	No
ALADIN63 (6h)	Model	CNRM	Era-Interim	0.11°	6	No
CNRM-RCSM4	Model	CNRM	Era-Interim	0.45°	3	Yes
RegCM4-6 (3h)	Model	ICTP	Era-Interim	0.11°	3	No
RegCM4-6 (6h)	Model	ICTP	Era-Interim	0.11°	6	No

REMO is a regional atmospheric climate model developed by the German Max Planck Institute. It is available at high spatial (around 24 kilometres) and temporal resolutions (3-hourly data) (Jacob et al., 2012; de la Vara et al., 2021). REMO can be coupled with the Max Planck ocean model MPIOM to obtain an atmosphere-ocean coupled regional climate model (MPIOM-REMO) also with 24 km grid spacing and 3-hourly data (Mikolajewicz et al., 2005; Elizalde et al., 2014; Sein et al., 2015; Cabos et al., 2019, 2020; Sein et al., 2020). Both REMO and MPIOM-REMO are forced by ERA-Interim reanalysis for the evaluation period (Sein et al., 2015, 2020; de la Vara et al., 2021) and by MPI-ESM-LR global model (Giorgetta et al., 2013) from the Max Planck Institute to simulate the historical period and project the RCP8.5 emissions scenario (Sein et al., 2015, 2020).

ALADIN63 is a regional atmospheric climate model developed by the French National Centre for Scientific Research (CNRM). This model is obtained from the EURO-CORDEX database with a grid spacing of 12 kilometres and 3-hourly data. However, 6-hourly data are also available, from which the effect of temporal resolution can be studied (Radu et al., 2008; Sevault et al., 2014; Nabat et al., 2020). ALADIN63 can be coupled with NEMOMED8 regional ocean model to obtain a coupled regional climate model (CNRM-RCSM4). This model has been obtained from the Med-CORDEX web server with 3-hourly data and a spatial resolution of 50 kilometres (Sevault et al., 2014). Both simulations are forced by the ERA-Interim reanalysis for the evaluation period (Radu et al., 2008; Sevault et al., 2014). CNRM-RCSM4 is forced by CNRM global model CNRM-CM5 (Voldoire et al., 2013) to simulate the historical period and project the RCP8.5 emissions scenario (Reale et al., 2022).

Finally, RegCM4-6 is a regional atmospheric climate model developed by the Italian Abdus Salam International Centre for Theoretical Physics (ICTP). Like ALADIN63, it was obtained from the EURO-CORDEX database with a grid spacing of 12 km and 3-hourly data, but its 6-hourly temporal resolution has also been investigated (Pal et al., 2007; Gu and Wang, 2020). RegCM4-6 is forced by the ERA-Interim reanalysis for the evaluation period (Gu and Wang, 2020).

2.2. Reanalysis data

In this work, ERA5 (Hersbach et al., 2020) reanalysis was chosen to compare with model data (and also against another reanalysis product, to show the spread among these type of datasets). Despite its lower resolution, ERA5 satisfactorily describes many wind characteristics (Jourdier, 2020), such as the main observed climatic wind features over the continent (Molina et al., 2021). ERA5 presents hourly data at a horizontal resolution of 31 kilometres. It was extracted from the

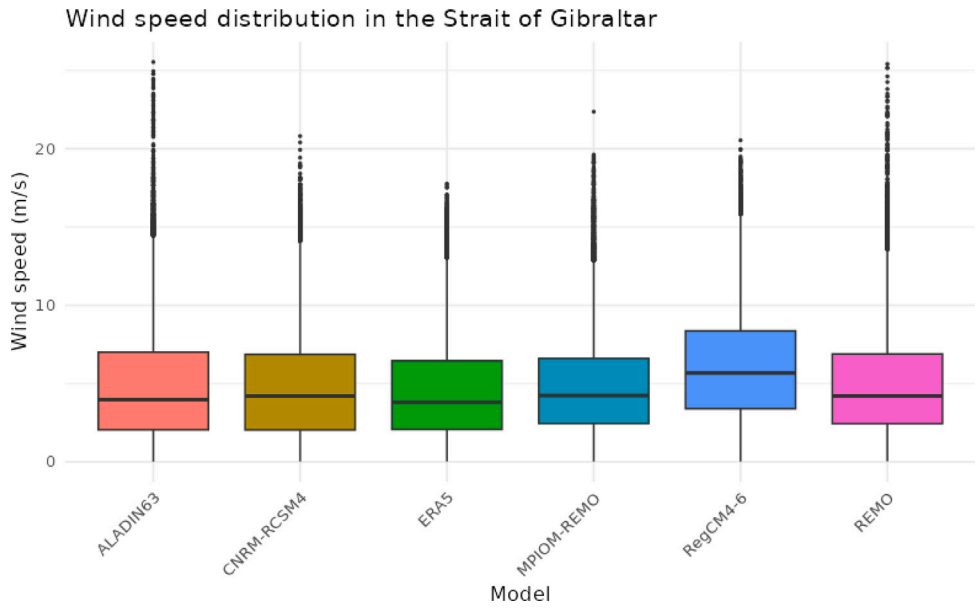

Fig. 1. Wind speed distribution in the Strait of Gibraltar for all models (3-hourly frequency) and ERA5 reanalysis (1-hourly frequency).

Copernicus Climate Change Service (C3S), specifically its Climate Data Store (https://cds.climate.copernicus.eu/cdsapp#!/dataset/reanalysis-era5-single-levels).

COSMO-REA6 reanalysis (Bollmeyer et al., 2015) is one of the highest resolution reanalyses available (6 kilometres, hourly data). Ortega et al. (2023, 2024) concluded that COSMO-REA6 is capable of adequately representing peninsular regional winds.

2.3. Study domains

The marine geographical Strait of Gibraltar demarcation has been considered as a sufficiently wide region that covers the entire area where the conditions that define regional winds can potentially occur. The RCMs simulation domain extends enough to east and west directions to capture flows that also affect southern Andalusia, Portugal and North Africa coasts. The geographic boundaries of the domain will depend on the spatial resolution of the different reanalyses and models. The domains are shown in Appendix A, Fig. A.15.

2.4. Levante and poniente definitions

Levante is characterized as easterly winds exceeding 5.5 m/s for at least 12 h in 20% of the domain area. Similarly, Poniente is characterized as westerly winds exceeding 5.5 m/s for at least 12 h in 20% of the domain area.

Speed threshold (5.5 m/s) is based on Ortega et al. (2023), while the direction thresholds (easterly component for Levante and westerly component for Poniente) extend direction range similarly to Ortega et al. (2024). The main concern of this work is to perform a consistent analysis for these flows, that is, under the same parameters and analysis than previous literature (Obermann et al., 2018; Obermann-Hellhund and Ahrens, 2018; Obermann-Hellhund et al., 2018). This analysis depends on the one published by Ortega et al. (2023), which it aims to extend.

Values between 5 and 6 m/s are common in named winds (Tout and Kemp, 1985), which, with some exceptions (Ortega et al., 2024), tend to be quite intense. When observing wind speed distribution in the Strait of Gibraltar (Fig. 1), most models, as well as ERA5, have mean wind speeds below 5 m/s. Thus, the threshold is considered to be moderate enough to capture high-intensity flows. The only exception is RegCM4-6 model, whose mean speeds and percentiles show much higher values. This is consistent with results below.

In addition, a Levante or Poniente day is considered when at least twelve hours in which the criteria of intensity and area are met. Extension is a very useful parameter when describing regional winds, as it is also an indicator of their intensity. Previous articles (Ortega et al., 2023, 2024) show that they do not always extend in the same way on a given day. Therefore, extension can be added as a threshold to consider a day on which that regional wind manifests itself with sufficient intensity in the area where it appears. Since Levante and Poniente have been characterized in previous studies (Ortega et al., 2023), and since station-based thresholds were not available here as in that paper, a statistical analysis to select a minimum extension percentage for the evaluation period, such that the results for Levante and Poniente days were consistent with those found in the literature, was performed. Thus, thresholds are proposed to obtain a robust statistic, similar to the small amount of available observations, following the analysis performed in Ortega et al. (2023, 2024).

2.5. Data analysis

Zonal and meridional wind components at surface level (10 m) provided wind speed and direction, while mean sea level pressure was used to obtain pressure anomalies in the common evaluation period (1995–2011) for all models and reanalyses. These variables are also used in the historical period (1950–2005) and the RCP8.5 emissions scenario (2006–2099) to inspect climate change signals.

Seasonal analyses, Pearson correlation coefficient, centred root mean square error (CRMSE) and standard deviation have been calculated for each reanalysis against each model in the common evaluation period (1995–2011). This way, the degree of agreement of all simulations with ERA5 and COSMO-REA6 can be analysed. CRMSE is defined as follows: $CRMSE = \sqrt{\frac{\sum_{i=1}^{n}((m_i-\bar{m})-(r_i-\bar{r}))^2}{N}}$, where N is the number of steps in the time series, m denotes the values given by the regional climate model and r marks the reference reanalysis data. All these statistics have been represented by a Taylor diagram (Taylor, 2001).

Levante and Poniente days were obtained for all simulations and reanalysis. Their annual cycles, temporal evolution, trends (for which a Mann–Kendall test (Mann, 1945; Kendall, 1948) was used with a significance level α=0.05), coefficients of variation (CV, the proportion between the standard deviation and the mean: $cv = \sigma/\mu$) and the distribution of their extension percentages for all periods were described. In addition, nonparametric Mann–Whitney–Wilcoxon (MWW) mean rank

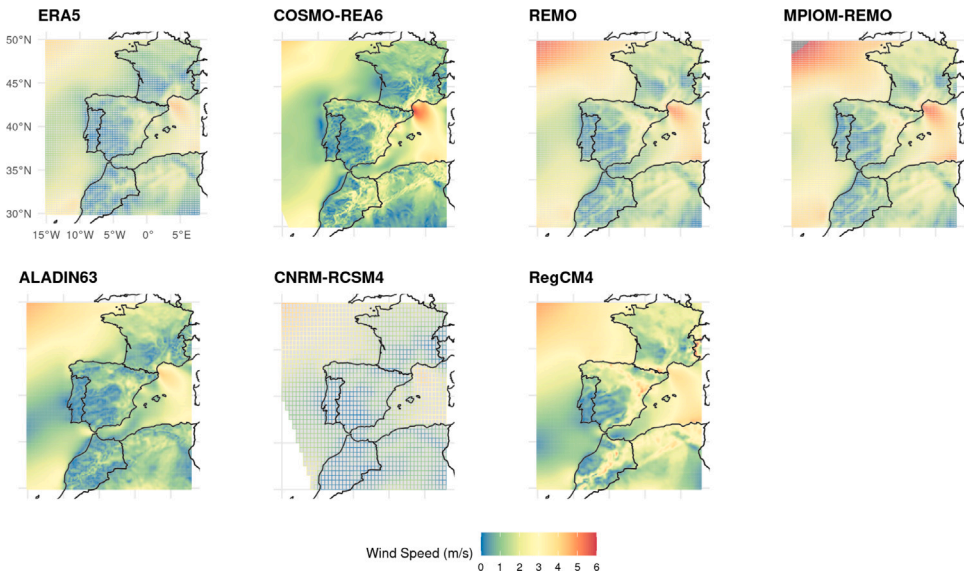

Fig. 2. Mean winter (DJF) wind speed (in m/s) over the Iberian Peninsula during the common evaluation period (1995–2011) of two reanalyses (ERA5 and COSMO-REA6) and regional climate models (REMO, MPIOM-REMO, ALADIN63, CNRM-RCSM4 and RegCM4-6).

difference test (Mann and Whitney, 1947), which does not assume data normality, was used to analyse statistical differences between some model pairs over the evaluation period, with a significance level α=0.05.

Results for the historical period (1950–2005) were compared with those of RCP8.5 future projection emissions scenario (2006–2099).

Given the difference in length between periods, all these calculations were carried out both for the complete periods and for 25-year subperiods. However, we found that the conclusions in most calculations when these separations were taken into account were equivalent to those when they were not, undoubtedly due to the high intensity of these flows and the slight changes they undergo. The differences between subperiods will be explained in the text whenever necessary.

Finally, weather regimes that explain 85% of the variance in both periods were obtained, and the predominant patterns for the days of appearance of each regional wind were investigated. Weather regimes (WRs) are large-scale recurring weather patterns (Garrido-Perez et al., 2020). An objective method to define WRs is to create clusters so that atmospheric fields that are very similar to each other are grouped by means of Empirical Orthogonal Functions (EOFs) (Vrac and Yiou, 2010). A k-means algorithm (Vrac and Yiou, 2010) was used to distribute every wind day to each cluster. The domain chosen to perform the analysis is the one closest to Ortega et al. (2023), since in this work a similar methodology was used to study Levante and Poniente weather regimes in the present period.

3. Results

3.1. Regional model evaluation (1995–2011)

3.1.1. Mean wind speed spatial distribution

Models correspond adequately with reanalysis data. Between ERA5 and COSMO-REA6, the differences are, for example, on the intensities in the Atlantic or the Gulf of Lion, as higher resolution allows for representing more details about the flows. In winter months (Fig. 2), REMO and MPIOM-REMO present mean wind speed fields of around 6 m/s in some places. In the inner Peninsula, both models show a higher speed on the Mediterranean and Cantabrian coasts (4–5 m/s) than inland (2–3 m/s). ALADIN63, although it broadly shares these characteristics, simulates a higher intensity on the western Strait coast. CNRM-RCSM4 underestimates wind intensity in the inner Peninsula. Finally, RegCM4-6 describes similar wind patterns to REMO and ALADIN63, with even higher values. Comparison of RCMs against reanalysis presents many aspects of similarity on the main wind structures. However, some differences are also obtained, such us REMO and MPIO-REMO in the northern offshore area.

As for summer winds, Fig. 3 shows a lower mean wind speed than in winter (Fig. 2), as expected (Ortega et al., 2023). RCMs generally simulate a higher wind speed on the Atlantic coast (around 5 m/s) than on the Mediterranean coast (3–4 m/s) and inland (1–2 m/s). All simulations and reanalyses present summer means that are much more homogeneous than winter means. REMO and MPIOM-REMO are similar to each other and show particular distributions of the mean field in the Alboran Sea. On the other hand, in summer the differences are of local nature: in ALADIN63 and in CNRM-RCSM4 a positive bias is seen in the area where Mistral appears. When compared with reanalysis data, ALADIN63 is particularly close to ERA5 in its marine characteristics; REMO and MPIOM-REMO, in their terrestrial characteristics.

All models have been statistically evaluated using a Taylor diagram (Fig. 4) for the mean domain. ALADIN63 and CNRM-RCSM4 show a standard deviation close to 1 when compared with ERA5; REMO, MPIOM-REMO and RegCM4-4 show the same when compared to COSMO-REA6. CNRM-RCSM4, despite being the climate model with the lowest spatial resolution, is the closest model to both reanalyses. ALADIN63 presents very similar results. On the other hand, REMO and MPIOM-REMO return a good standard deviation when compared with ERA5, but their Pearson correlation coefficient is lower and their CRMSE is much higher. When compared with COSMO-REA6, results are similar except for the lower standard deviation. Finally, RegCM4-6 presents the highest standard deviation of all models for both reanalyses.

3.1.2. Main features of regional winds

Mean Levante extension (Table 2) is consistent for both reanalysis (always lower on average, varying by 37%–40% extension) and models (which usually fall within the range of 41%–45%). Similarly, Levante hours detected per day show that both reanalysis range around 16 h/day, meanwhile RCMs spread from 17–19, which is on average more than half of the day. Regarding the Levante days obtained, again, COSMO-REA6 is the reanalysis that best reproduces the available literature (Tout and Kemp, 1985; García de Pedraza, 1990; Lorente-Plazas et al., 2015; Hidalgo and Gallego, 2019; Ortega et al., 2023) with around 145 days per year. Levante frequency in reanalysis ranges

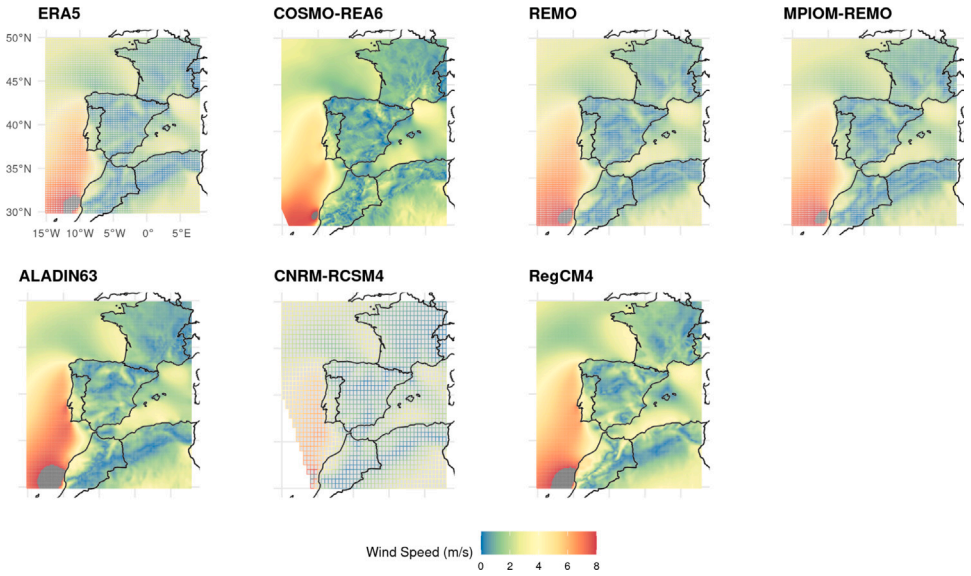

Fig. 3. Mean summer (JJA) wind speed over the Iberian Peninsula during the common evaluation period (1995–2011) of two reanalyses (ERA5 and COSMO-REA6) and regional climate models (REMO, MPIOM-REMO, ALADIN63, CNRM-RCSM4 and RegCM4-6).

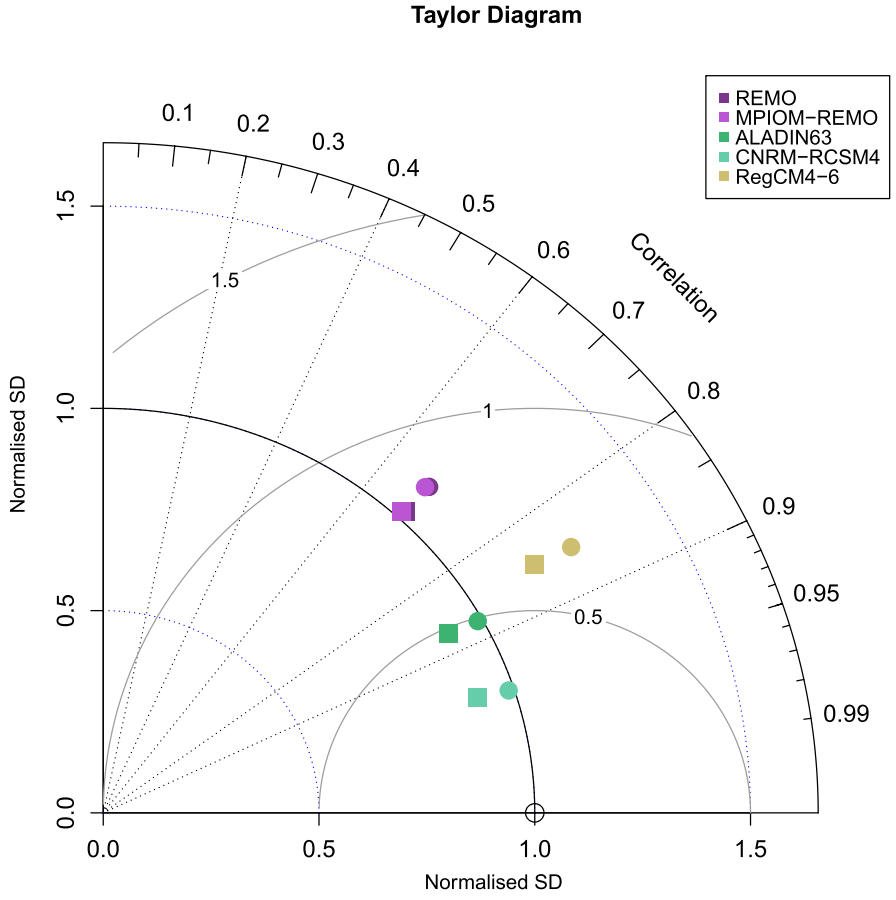

Fig. 4. Normalized Taylor diagram for the mean wind speed from regional climate models (REMO, MPIOM-REMO, ALADIN63, CNRM-RCSM4 and RegCM4-6) with respect to the ERA5 (circles) and COSMO-REA6 (squares) reanalyses in the common evaluation period (1995–2011). Pearson correlation coefficient is represented by the outer arc of the diagram; CRMSE, by the radial distance to the position of hypothetical perfect data; the percentage of the standard deviation between both time series, by the inner arcs. As it is a normalized Taylor diagram, the closer the CRMSE is to 0, and the closer the standard deviation and correlation are to 1, the better the simulations fit the reference.

from 122 to 144 days/year, while it is larger in RCMs ranging from 110 to 160 days/year.

Poniente shows, like Levante, extensions around half the proposed domain (Table 2). In this case, the only dataset that does not exceed

Table 2
Means and coefficients of variation (%) for percentage (%) extension, regional wind hours per day, and regional wind days per year from two reanalyses (ERA5 and COSMO-REA6) and regional climate models (REMO, MPIOM-REMO, ALADIN63, CNRM-RCSM4 and RegCM4-6) over the common evaluation period (1995–2011).

	LEVANTE						PONIENTE					
	Extension		Hours/Day		Days/Year		Extension		Hours/Day		Days/Year	
Model	Mean	CV	Mean	CV	Mean	CV	Mean	CV	Mean	CV	Mean	CV
ERA5	39.89	31.52	16.25	49.29	122.35	12.65	41.75	33.05	16.78	47.84	168.76	10.65
COSMO-REA6	37.05	33.51	15.40	52.71	144.76	13.06	39.43	34.23	15.72	53.08	120.12	12.79
REMO	42.04	32.07	17.47	42.80	120.12	14.15	44.41	34.37	17.06	46.52	130.76	11.75
MPIOM-REMO	43.24	31.66	17.89	41.49	129.76	8.57	44.54	34.10	17.15	45.43	128.94	12.04
ALADIN63 (3 h)	41.01	32.47	17.74	41.67	141.88	12.66	41.57	34.02	16.52	47.31	107.88	13.21
ALADIN63 (6 h)	41.05	32.38	18.40	37.23	152.82	11.05	41.58	33.90	17.10	43.52	113.29	12.72
CNRM-RCSM4	42.17	32.68	17.97	40.98	112.00	15.91	41.17	35.14	17.18	44.85	131.47	13.84
RegCM4-6 (3 h)	45.08	31.41	18.96	37.09	150.71	12.57	45.98	33.67	17.52	43.99	138.59	13.48
RegCM4-6 (6 h)	45.06	31.39	19.61	32.53	157.65	12.28	46.01	33.61	18.06	40.06	144.00	14.44

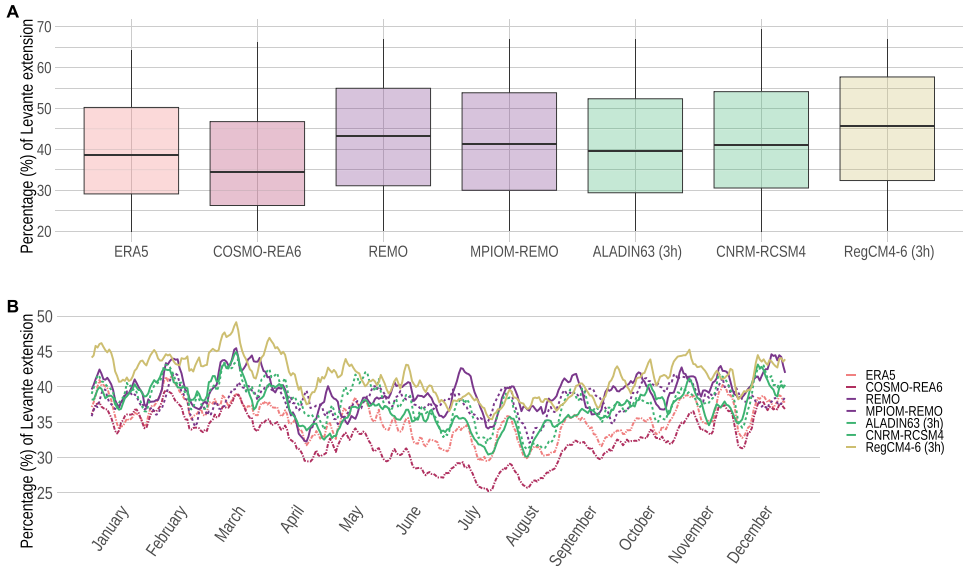

Fig. 5. Distribution (A) and annual cycle with sub-daily data smoothed by a 10-day moving window (B) of Levante percentage extension according to two reanalysis and RCMs in the common evaluation period (1995–2011). Uncoupled models show solid lines; coupled models, dashed lines.

40% of the average extension percentage is COSMO-REA6. The simulation closest to COSMO-REA6 is the ALADIN63/CNRM-RCSM4 pair, with the rest overestimating the area up to 45%–46%. The values are consistent with the results of Ortega et al. (2023), in which Levante and Poniente extensions reach similar magnitudes. For Poniente hours per day, all models overestimate the results of COSMO-REA6. The coefficients of variation, in this case, are much higher, demonstrating the great natural variability of this wind. Regarding the number of Poniente days per year, the methodology generally overestimates it. The closest appears to be ALADIN63, followed by COSMO-REA6 and REMO/MPIOM-REMO and CNRM-RCSM4.

3.1.3. Regional wind events

Before addressing the issue of the number of regional wind events detected, the captured extension must be studied, since it is one of the thresholds that determines the number of days in which a wind event appears.

Levante extension percentages (Fig. 5, A) are similar to each other, although all models overestimate COSMO-REA6 reanalysis (25%–45%); they present extensions in the 30%–55% range. All models detect Levante in more than 20% of the Strait during most hours. For the medians, ALADIN63/CNRM-RCSM4 and REMO/MPIOM-REMO pairs are the most similar to COSMO-REA6 and ERA5. Annual cycles of Levante percentage extension (Fig. 5, B) are quite similar for all models, with ALADIN63 and CNRM-RCSM4 being the most similar to COSMO-REA6, followed by the REMO/MPIOM-REMO pair. RegCM4-6 is the model furthest from the reanalyses, presenting greater overestimation of Levante percentage extension.

COSMO-REA6 distribution of Poniente percentage extension (Fig. 6, A) moves in a range of 38%–50%, with medians around 36%. Models overestimate it: ALADIN63 and CNRM-RCSM4 show a range of 30%–55% (medians in the 40%), while REMO, MPIOM-REMO and RegCM4-6 show a range of 30%–60% (medians in the 45%). It seems that Poniente appears around 40% of the Strait on most days. The distribution is quite similar to that of Levante (Fig. 5, A). As for the annual cycle of Poniente percentage extension (Fig. 6, B), this is adequately identified with Ortega et al. (2023) for all models. Although simulations overestimate the results of COSMO-REA6, REMO/MPIOM-REMO and ALADIN63/CNRM-RCSM4 couples reproduce ERA5 results.

Models also show the ability to simulate the alternation of Levante and Poniente events. Thus, REMO/MPIOM-REMO pair reproduces in its daily means that, when Poniente appears, Levante usually does not, and vice versa (Fig. 7). This calculation was carried out in Ortega et al. (2023) when describing offshore winds. REMO and MPIOM-REMO overestimate Levante in summer, but models are capable of reproducing flow alternation.

Reanalysis medians of Levante hours per day (Fig. 8, A) are between 15 (COSMO-REA6) and 20 (ERA5) hours. RCMs are in general closer to ERA5 values. For Levante, REMO/MPIOM-REMO and ALADIN63 behave appropriately, while CNRM-RCSM4, which otherwise reproduces the distributions, underestimates the number of Levante wind days (Table 2). The annual cycle of monthly Levante days (Fig. 8, B)

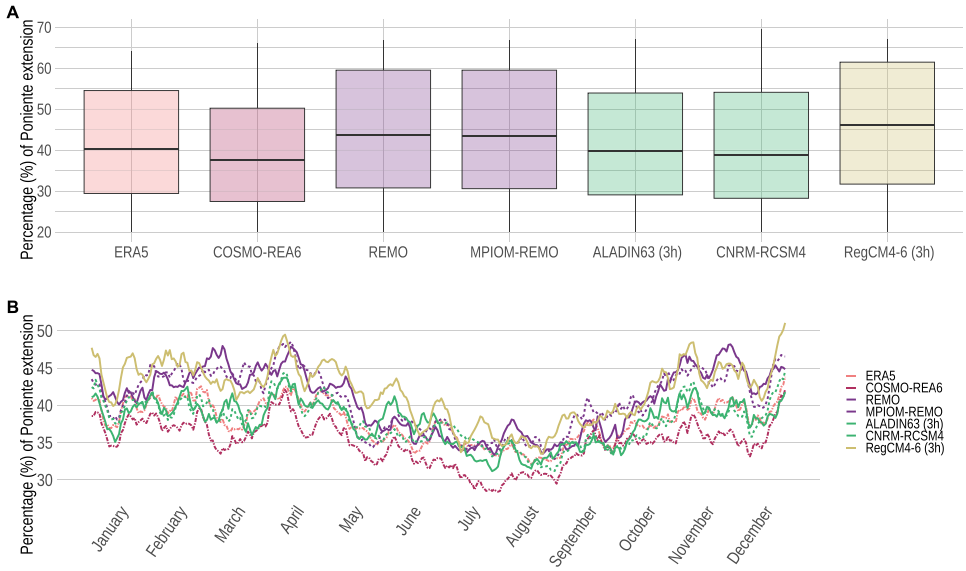

Fig. 6. Distribution (A) and annual cycle with sub-daily data smoothed by a 10-day moving window (B) of Poniente percentage extension according to two reanalysis and RCMs in the common evaluation period (1995–2011). Uncoupled models show solid lines; coupled models, dashed lines.

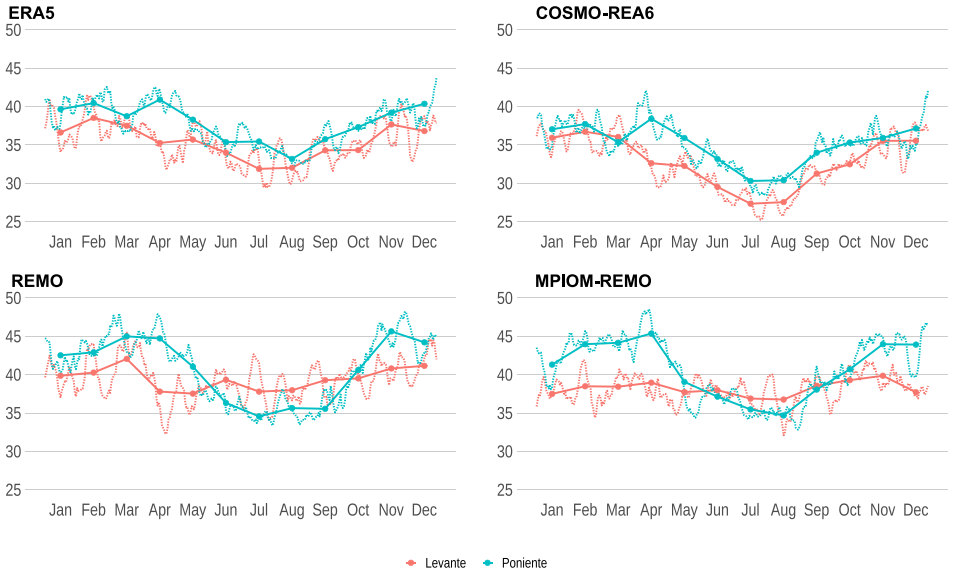

Fig. 7. Annual cycles of Levante and Poniente percentage extensions through monthly means (solid line) and daily means smoothed by a 10-day moving window (dashed line) for ERA5 and COSMO-REA6 reanalyses and regional climate models REMO and MPIOM-REMO in the common evaluation period (1995–2011).

exhibits a spread among RCMs similar to the one seen between both reanalyses, with more consistency on winter and spring months (such as January-March maximum) and larger differences during summer months.

The distribution of Poniente hours per day (Fig. 9, A) for COSMO-REA6 shows a greater range than that of Levante: 7–24 h, with medians of 17 h per day. ERA5, REMO, MPIOM-REMO and CNRM-RCSM4 slightly overestimate the range (9–24 h, with medians of 21–22 h). ALADIN63 overestimates the range (9–24 h) but reproduces the median (18 h) better. It seems that ALADIN63/CNRM-RCSM4 and REMO/MPIOM-REMO pairs fit the reanalysis products. For the annual cycle of monthly Poniente days (Fig. 9, B), although a sharp decrease in Poniente days is observed in October, these do not remain stable in the rest of the months. COSMO-REA6 reproduces a slight increase in spring, while in ERA5 it occurs in spring and summer. REMO and MPIOM-REMO adequately simulate the spring increase of COSMO-REA6, as well as the summer increase of ERA5 to a much lesser extent. ALADIN63 is more similar to COSMO-REA6, although it delays the increase in days to late spring and early summer. CNRM-RCSM4 imitates the distribution of ERA5.

Finally, the influence of model temporal resolution and coupling effect on regional wind modelling has also been studied. Results suggest that temporal resolution does not seem to affect the extension of Levante and Poniente winds. However, 3h/6h model pairs are not able to obtain the same regional wind hours per day, since the 6-hourly version is much less similar to reanalysis and literature references. For this reason, only the version with 3-hourly data has been considered in the study of extension and events. Calculations referring to temporal resolution can be consulted in Appendix B (Figs. B.16–B.19). On coupling effects, results vary greatly depending on the regional wind studied, that is, depending on its spatial structures and its greater or lesser marine influence. These calculations can also be found in Appendix C (Figs. C.20–C.21).

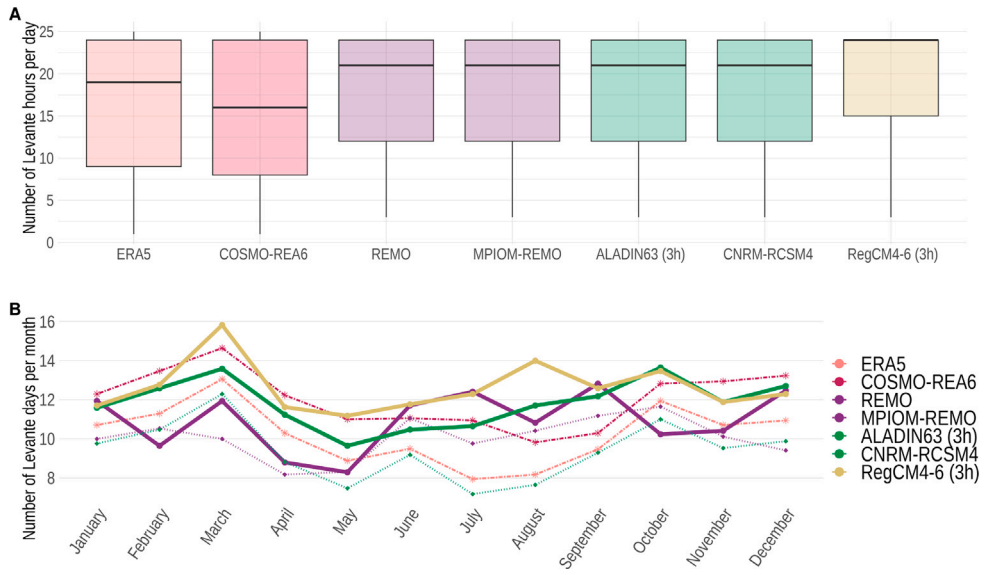

Fig. 8. Distribution of Levante daily hours (A) and annual cycle of the monthly number of days (B) according to two reanalysis and RCMs in the common evaluation period (1995–2011). Uncoupled models show solid lines; coupled models, dashed lines.

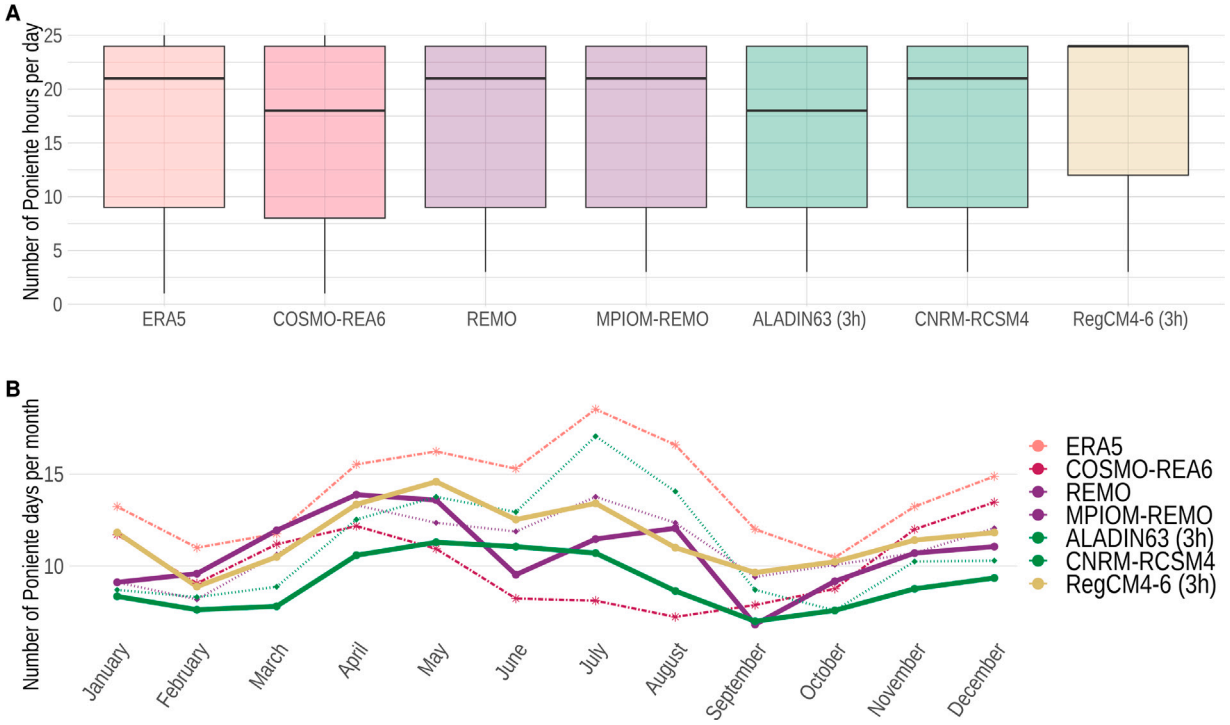

Fig. 9. Distribution of Poniente daily hours (A) and annual cycle of the monthly number of days (B) according to several climate models in the common evaluation period (1995–2011). Uncoupled models show solid lines; coupled models, dashed lines.

3.2. Future climate regional winds projections assessment

Climate change projection analysis will focus on REMO, MPIOM-REMO, and CNRM-RCSM4 models, as they adequately represent regional winds and their data was available in the described sources at the time of elaboration.

3.2.1. Levante

Mean Levante extension (44%) and daily hours (18 hours/day) exhibit quite similar values for future projections compared to the historical period (Table 3). In all three models, more days are captured in the future period than in the historical period.

The annual cycle of Levante extension (Fig. 10, A) is not strong, with some differences among RCMs. REMO detects a very marked summer rise that the other models do not capture it. MPIOM-REMO and CNRM-RCSM4 obtain a greater decrease in the percentage of extension from April onwards. The three models show an increase in Levante days between spring and summer (Fig. 10, B). Thus, all detect a minimum of 6–10 days at the end of autumn, winter and early spring, an increase around May–June, a maximum between July and September and a new decrease at the beginning of autumn.

Time series of Levante extension and days (Fig. 11) are quite noisy, due to the well-known natural variability of wind on climatic scales. REMO detects a 1% increase in the extension in the third quarter of the

Table 3
Averages and coefficients of variation (%) for the percentage (%) of extension, regional wind hours per day and regional wind days per year according to the regional climate models REMO, MPIOM-REMO and CNRM-RCSM4 in the historical period (1950–2005) and the future projection under the RCP8.5 emissions scenario (2006–2099).

HISTORICAL PERIOD (1950–2005)												
	LEVANTE						PONIENTE					
	Extension		Hours/Day		Days/Year		Extension		Hours/Day		Days/Year	
Model	Mean	CV	Mean	CV	Mean	CV	Mean	CV	Mean	CV	Mean	CV
REMO	44.35	31.44	17.89	40.97	130.86	14.57	48.17	32.21	17.54	44.72	143.07	13.62
MPIOM-REMO	42.85	32.09	17.49	42.61	125.05	13.46	46.14	33.48	17.13	46.52	136.16	14.13
CNRM-RCSM4	42.74	32.82	17.77	41.93	110.45	16.58	44.66	34.04	18.13	41.51	156.16	12.83
RCP8.5 EMISSIONS SCENARIO (2006–2099)												
	LEVANTE						PONIENTE					
	Extension		Hours/Day		Days/Year		Extension		Hours/Day		Days/Year	
Model	Mean	CV	Mean	CV	Mean	CV	Mean	CV	Mean	CV	Mean	CV
REMO	44.22	31.15	18.08	40.43	137.52	14.75	46.69	33.35	17.17	46.04	135.51	14.17
MPIOM-REMO	42.66	31.58	17.85	41.28	128.32	14.09	45.09	34.32	17.02	46.68	131.18	13.22
CNRM-RCSM4	42.95	32.31	18.17	39.95	120.21	15.69	43.44	34.61	17.81	42.89	147.53	13.21

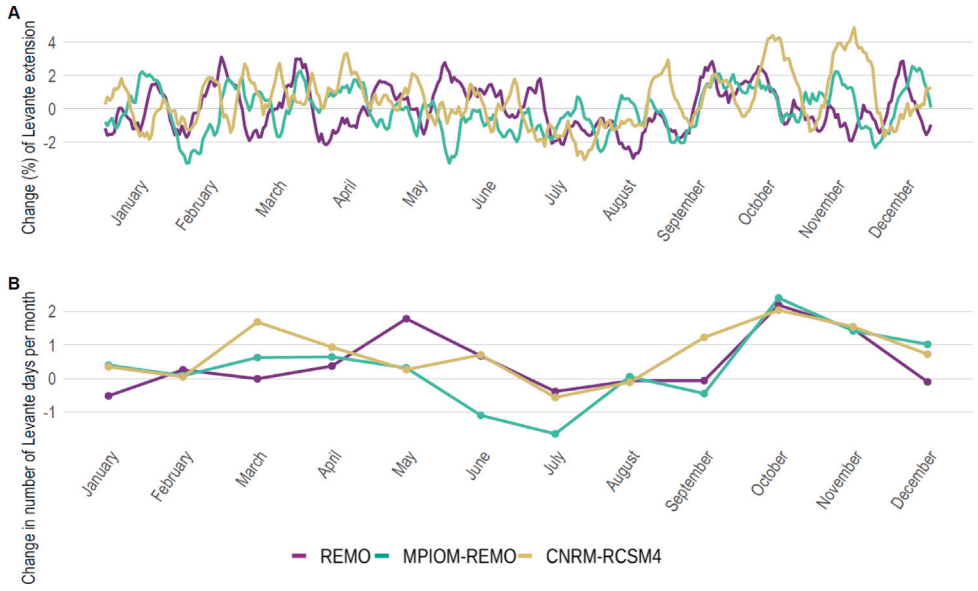

Fig. 10. Changes (future period, 2006–2099, minus historical period, 1950–2005) in the annual cycle of Levante extension percentage (A) and Levante monthly days (B) according to the regional climate models REMO, MPIOM-REMO and CNRM-RCSM4.

20th century, but decreases a 2%–3% in the first and last quarters of the 21st century. On the other hand, MPIOM-REMO shows a decrease in Levante extension for both periods and all subperiods, except the first quarter of the 21st century, where the trend is slightly upward. In this case, the most relevant decreases are those of the quarters 2025–2050 and 2075–2099, of 2%–3%, reaching a minimum annual Levante extension of 40% of the Strait on average. Finally, CNMR-RCSM4 shows upward trends in both periods; although in the quarters 2000–2025, 2050–2075 and 2075–2099 they are slightly downwards, they are compensated by the strong rise of the quarter 2025–2050, where it rises from less than 40% to the usual 43%. These trends are significant according to the Mann–Kendall test (Appendix D, Table D.5).

Trends for annual Levante days (Fig. 11) are similar for all models. They show stability in the historical period and a small decrease of 2–4 days in the third quarter of the 20th century. However, the three models obtain positive trends in future projections, although the magnitude of the change is more intense for CNRM-RCSM4 (10 days) than for REMO and MPIOM-REMO (around 5 days). This is due to the strong increase in days detected by CNRM-RCSM4 in the 2025–2050 and 2075–2099 quarters, which the other models do not detect and even reproduce with a negative sign. Of all these trends, only that of CNRM-RCSM4 projection is statistically significant (Appendix D, Table D.5). Overall, all three models agree that the number of detected Levante days will increase over the 21st century to around 120–140 days per year, by a magnitude of 10–20 events.

3.2.2. *Poniente*

Future projections for Poniente (Table 3) show an annual days decrease lower than 5%.

The annual cycle of Poniente extension percentage (Fig. 12, A) is very marked. It coincides for the three models, with a clear summer decrease (about 35% of the Strait) and a maximum in winter (around 50% of the Strait). However, no major differences are seen between the periods. The case of the annual cycle for detected Poniente days (Fig. 12, B) is different. REMO and MPIOM-REMO show a decrease in Poniente days in May, a minimum in September (around 8 days per month) and maximums from December to April (about 15 days). The CRNM cycle is slightly different, as large spring values are extended up to June.

There is less coincidence for the extremes between CNRM-RCSM4 and the REMO/MPIOM-REMO pair (Fig. 13). Both MPIOM-REMO and CNRM-RCSM4 show stable trends in the historical period, while REMO

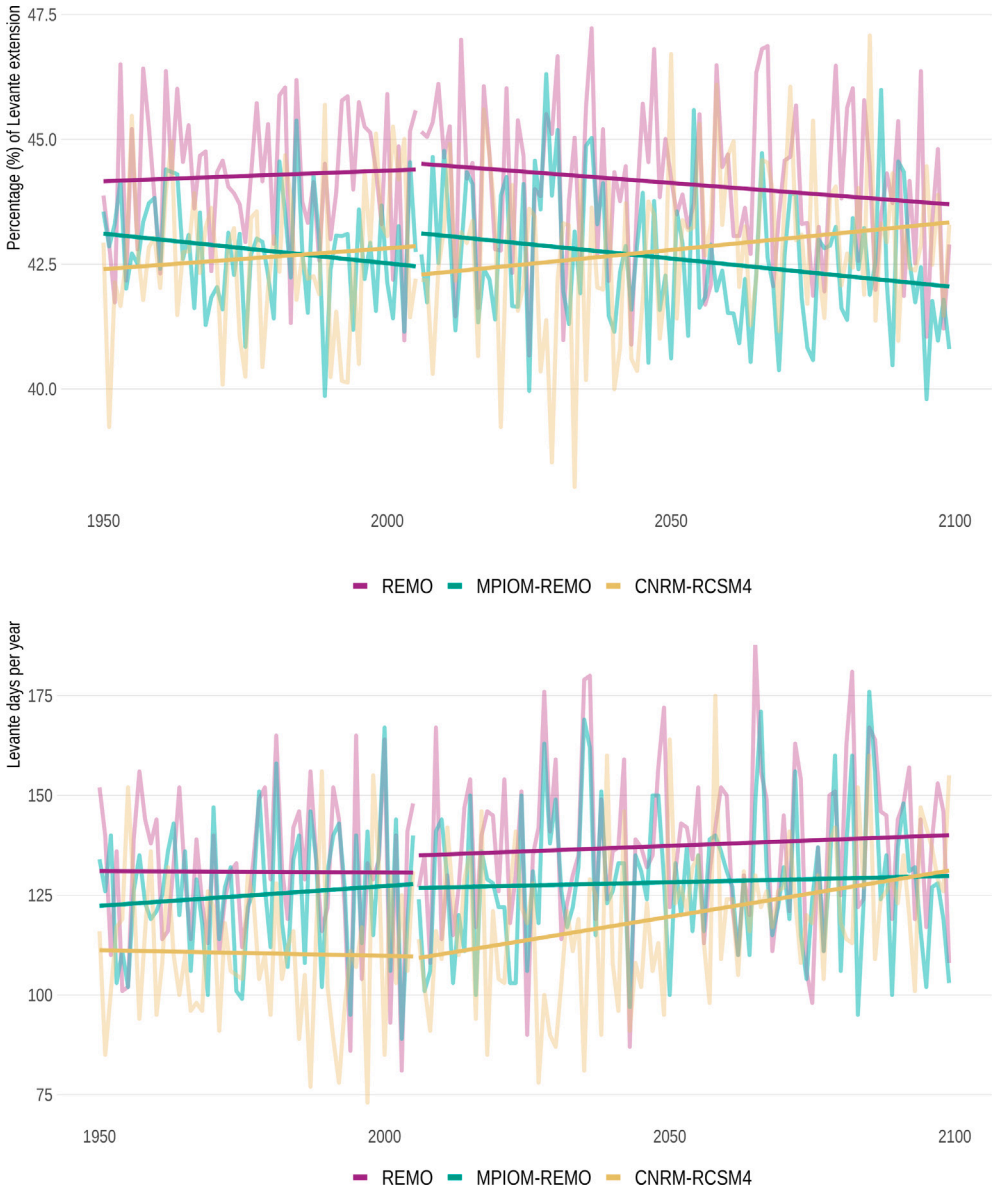

Fig. 11. Time series for Levante extension (A) and Levante days (B) for historical (1950–2005) and RCP8.5 emissions scenario (2006–2099) according to the regional climate models REMO, MPIOM-REMO and CNRM-RCSM4.

returns a slightly positive trend. In any case, the three models return strong downward trends in the historical period with a magnitude of approximately 3%–5% extension (from 44%–47% to 42%–46%). When dividing the projection into 25-year subperiods, this decrease is visible for CNRM-RCSM4 and more irregular for the other two. These trends are significant for the three models (Appendix D, Table D.5).

The agreement between models on the trend of annual Poniente days detected in the Strait in both periods (Fig. 13) is somewhat lower. In the historical period both MPIOM-REMO and REMO detect a negative trend, while that of CNRM-RCSM4 is positive. These signs are contrary when dividing the historical simulation into 25-year subperiods. However, none of the trends is significant (shown in Appendix D, Tables D.6 and D.7). In the future projection, the three models agree that the trend is negative and comparable. As in the case of the extension, these results are extensible to the division into 25-year subperiods, except in the last quarter of the 21st century. Finally, only the trend of the CNRM-RCSM4 model is significant. This decrease would have a magnitude of about 5–20 days, depending on the model.

3.2.3. *Weather regimes*

Finally, a brief study of the weather regimes that can give rise to these regional winds was conducted to provide an overview of the potential dynamics of these phenomena. Using REMO, MPIOM-REMO and CNRM-RCSM4 models, whose historical and future projections were analysed, only three EOFs (Empirical Orthogonal Functions) were obtained, reflecting 85% of the variance of the periods studied (Fig. 14, for 1950–2005 and 2006–2099). These results have attempted to approximate to the evaluation carried out in Ortega et al. (2023) with COSMO-REA6.

As can be seen in Fig. 14, all three models agree with the study conducted in Ortega et al. (2023) in that the main weather regime presents an anticyclonic anomaly over the British Isles and northern Europe, which we will call WR1 (EOF1 for both REMO historical periods and MPIOM-REMO projections; EOF2 for REMO projections; EOF3 for CNRM-RCSM4), and a configuration with large pressure differences between western and eastern Europe, which we will call WR2 (EOF2 for both historical periods, EOF1 for REMO projections and CNRM-RCSM4,

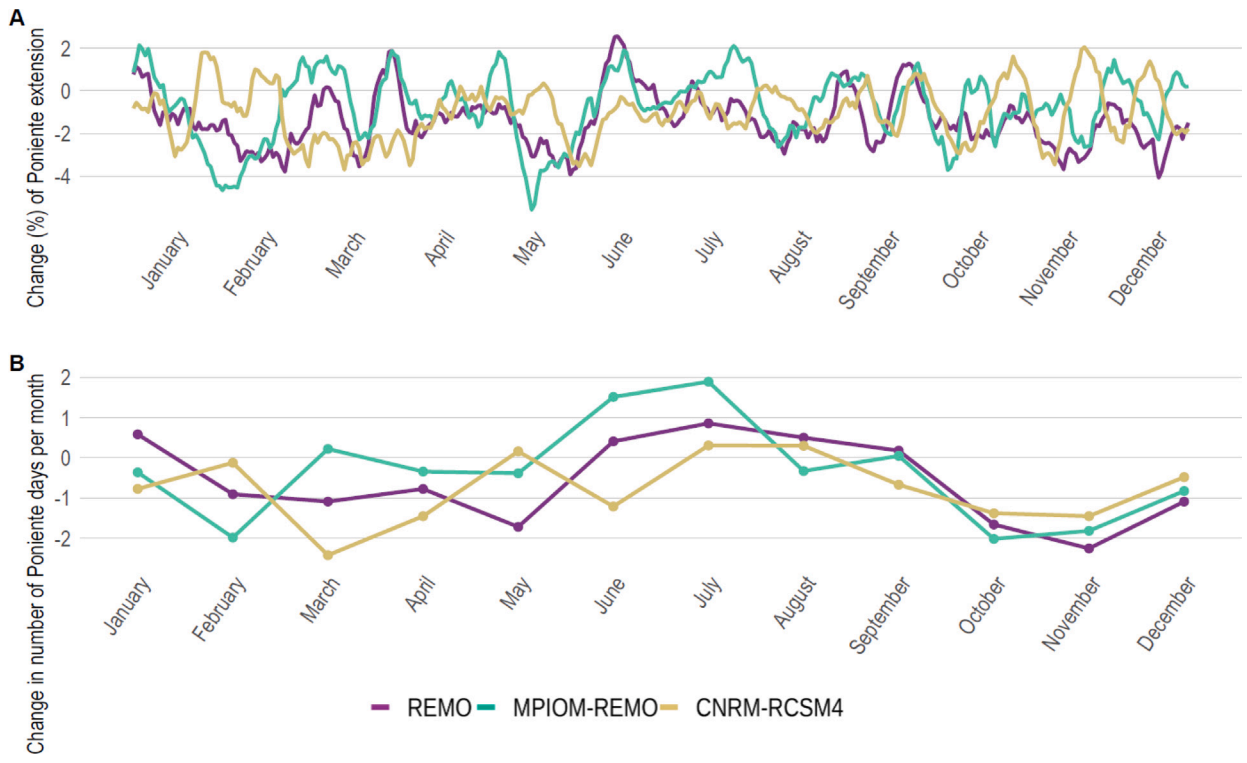

Fig. 12. Changes (future period, 2006–2099, minus historical period, 1950–2005) in the annual cycle of Poniente extension percentage (A) and Poniente monthly days (B) according to the regional climate models REMO, MPIOM-REMO and CNRM-RCSM4.

Table 4
Distribution (%) of total Levante and Poniente days in annual weather regimes (Fig. 14) according to REMO, MPIOM-REMO and CNRM-RCSM4 models.

HISTORICAL PERIOD (1950–2005)						
	LEVANTE			PONIENTE		
WR	REMO	MPIOM-REMO	CNRM-RCSM4	REMO	MPIOM-REMO	CNRM-RCSM4
WR1	34.65	36.76	38.79	41.04	46.52	46.78
WR2	58.72	54.25	57.15	12.74	11.27	7.38
WR3	6.63	9.00	4.06	46.22	42.22	45.84
RCP8.5 EMISSIONS SCENARIO (2006–2099)						
	LEVANTE			PONIENTE		
WR	REMO	MPIOM-REMO	CNRM-RCSM4	REMO	MPIOM-REMO	CNRM-RCSM4
WR1	38.83	41.36	37.58	55.60	53.18	45.84
WR2	57.06	54.50	57.64	8.42	7.71	8.31
WR3	4.12	4.15	4.78	35.99	30.10	45.85

EOF3 for MPIOM-REMO projections). Furthermore, all models detect a third situation (WR3) of broad negative anomalies across Europe.

In the historical period, WRs for both REMO and MPIOM-REMO are very similar to those obtained in Ortega et al. (2023) for COSMO-REA6. In the future projected under RCP8.5 scenario, characteristics begin to diverge. First, in REMO WR2 takes on a clear predominance over WR1. MPIOM-REMO, while considering WR1 as the EOF with the highest percentage, has WR2 (with reversed sign) almost tied with WR3. CNRM-RCSM4, on the other hand, shows a predominance of WR2 over the other two situations and imperceptible changes between historical and future periods, but anomalies are more abrupt than for REMO and MPIOM-REMO.

There are no significant differences in the weather regimes over Europe throughout the 21st century for these models. These calculations have also been performed for future 50-year subperiods, so as to be comparable with the historical 50-year period, but the results did not show any differences and were unified for simplicity.

The distribution of the total Levante and Poniente days in each weather regime can be found in Table 4. In these distributions, however, it can be seen that the patterns that will generate the appearance of Levante and Poniente will be the same and in the same proportions. As for Levante, it seems to appear predominantly under WR2 situations on 55%–59% of the days in each period, but it also occurs in large numbers under WR1 (35%–42% of days). It rarely appears (always less than 10% of days) in WR3. On the other hand, Poniente consistently appears under WR1 (40%–55%) or WR3 (30%–45%). It very rarely occurs under WR2 (always less than 13%).

Of all obtained weather regimes, WR1 appears to be associated with a European Blocking configuration; WR2, with an Atlantic Ridge (Garrido-Perez et al., 2020; Ortega et al., 2024). As previously mentioned, these are very similar to those obtained by Ortega et al. (2023) for COSMO-REA6, with a similar domain. WR3 has no clear association with other regimes in the literature. It appears to be very similar to a NAO$^-$ situation in which the model domain does not allow for the simulation of the North Atlantic (Garrido-Perez et al., 2020), but it may also be due to the internal physics of the models. As in Ortega

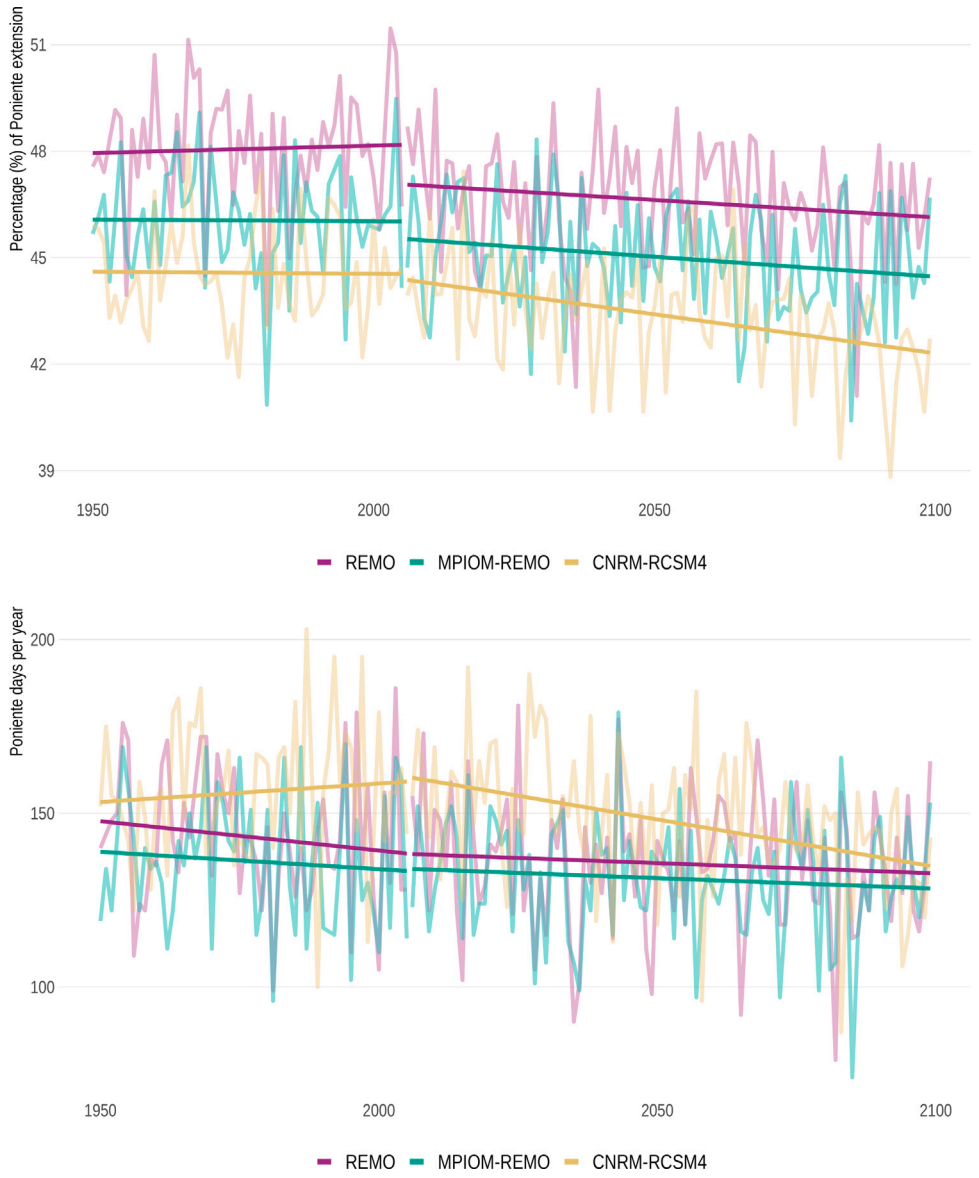

Fig. 13. Time series for Poniente extension (A) and Poniente days (B) for historical period (1950–2005) and RCP8.5 emissions scenario (2006–2099) according to the regional climate models REMO, MPIOM-REMO and CNRM-RCSM4.

et al. (2023), Levante is predominantly captured under WR1 and WR2 situations, although the models, unlike COSMO-REA6, usually find it under WR2 than WR1. Poniente winds occur primarily in situations other than the two described above, which was also the case in Ortega et al. (2023), although all models also find a high Poniente percentage under WR1. Since all three models find a high percentage of Levante winds under WR2 and that Levante and Poniente are contrary winds, there are few Poniente days under WR2 conditions.

4. Discussion

RCMs show 120–140 days per year of Levante, covering more than 40% of the Strait of Gibraltar (Table 2), and with an average duration of 20 h per day. Spatial extension exhibits a marked reduction during the summer months (Fig. 5, B). Frequency of events increases between January and March, followed by a decline from May onward (Fig. 8, B). Poniente is captured for around 120 to 167 days/year for reanalysis and 108 to 144 days/year for RCMs, and also extends on average around 40% of the Strait (Table 2). Poniente extension cycle (Fig. 6, B) varies in the monthly time series (Fig. 9, B), since this seems to depend on the location. There is a decrease around October, and most RCMs reproduce an increase in Poniente days between spring and summer. Although the overall description of the winds is similar to the literature, especially regarding Levante spatial extension and Poniente extension cycle (Ortega et al., 2023), some differences exist. For example, the range of Levante days is much narrower according to the models than the 80–165 days detected in previous observational studies (García-Bustamante et al., 2008; Ortega et al., 2023), while the number of Poniente events is twice that of García de Pedraza (1990).

REMO and MPIOM-REMO models are consistent in most of their characteristics. REMO is, inside EURO-CORDEX ensemble, one of the models with the least bias with respect to reanalysis data (Kunz et al., 2010; Winterfeldt et al., 2011; Vautard et al., 2021). MPIOM-REMO (Gualdi et al., 2013; Sein et al., 2015; Ruti et al., 2016) adequately describe various wind characteristics, such as mean values and gusts. ALADIN63 relates to reanalysis products and to the few available references better than REMO and MPIOM-REMO for Levante and Poniente main characteristics. CNRM-RCSM4, like ALADIN63, adequately describes Levante in the Strait of Gibraltar and agrees with reanalysis and other simulations in Poniente properties. Former evaluations have concluded that this model adequately simulates atmospheric

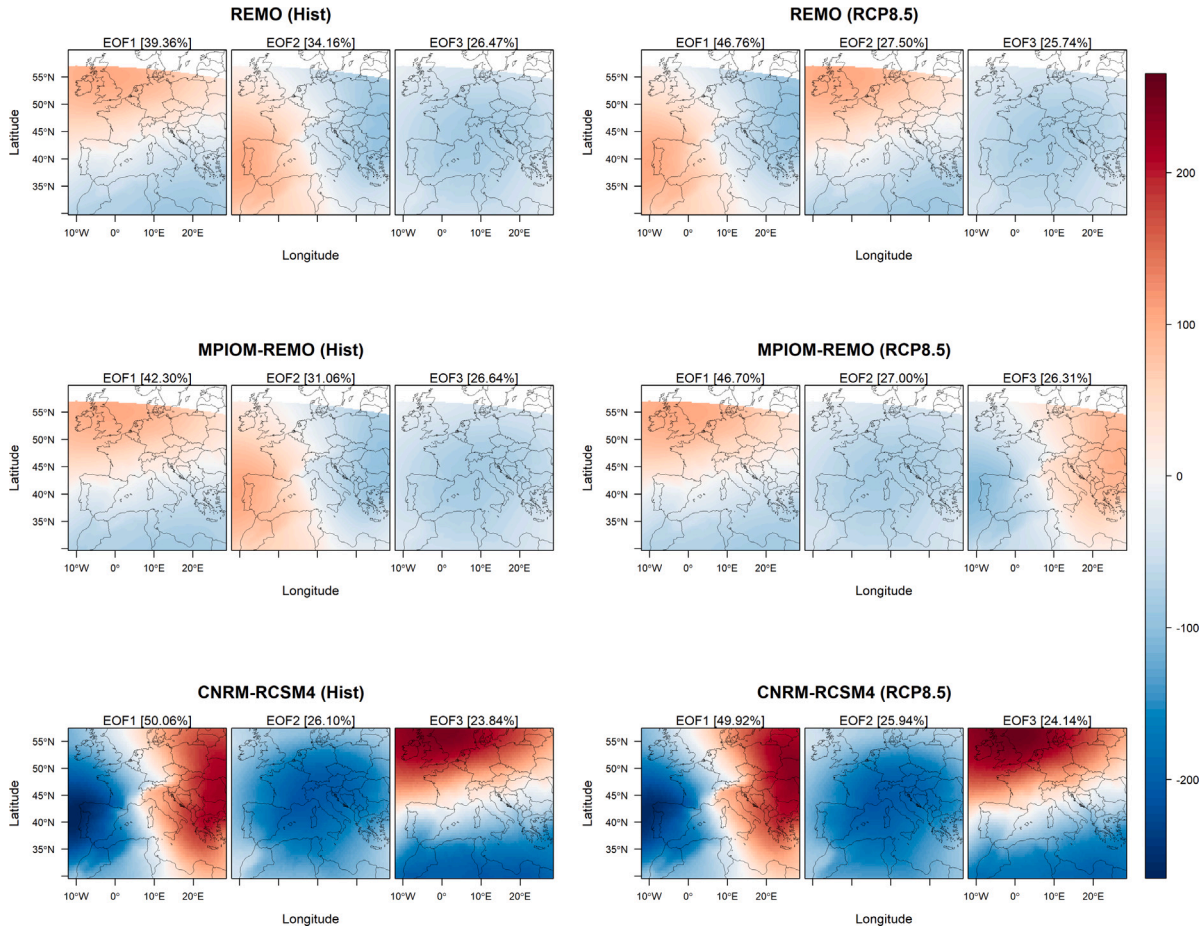

Fig. 14. EOFs for mean sea level pressure anomalies from REMO, MPIOM-REMO and CNRM-RCSM4 models (hPa) for the historical (1950–2005) and projected (2006–2099) periods. Daily data were used for the calculation.

variables (Sevault et al., 2014; Adloff et al., 2018; Gaertner et al., 2018; Vautard et al., 2021; Reale et al., 2022; Dunić et al., 2023), including wind speed (Sevault et al., 2014) and related properties such as the occurrence of Mediterranean cyclones (Gaertner et al., 2018; Reale et al., 2022). RegCM4-6 has difficulties in adequately representing the wind in multiple areas of the world (Maharana et al., 2019; da Silva et al., 2022; Xu et al., 2022). It is the furthest model from the reanalysis and the available references, but it has some strengths in representing these winds, such as higher correlation and lower CRMSE than REMO, and a wind flow intensity quite close to COSMO-REA6.

Model evaluation yields some general conclusions. (i) The product that seems closest to the references available in the literature (García de Pedraza, 1971, 1990; García de Pedraza and Reija, 1994; García de Pedraza and García Vega, 2001; Hidalgo and Gallego, 2019) is COSMO-REA6, with 6 kilometres of grid spacing. However, these references are very scarce; the first study similar to the present one is the one in Ortega et al. (2023), which also uses COSMO-REA6. (ii) Regarding studied models, REMO, MPIOM-REMO, ALADIN63 and CNRM-RCSM4 generally agree with the literature for Levante and Poniente flows, and therefore are of interest for the study of future projections.

Regional climate models detect no strong differences between historical period and future projections in Levante distributions and annual cycles. Levante frequency increases 10–20 annual events by the end of the 21st century under the RCP8.5 emissions scenario, in some cases in a statistically significant way (Fig. 11). The variation in its extension is also significant, but irregular and model-dependent. Some works indicate a possible future weakening for Strait winds, especially easterly winds, in summer (Gómez et al., 2016), while others project an increase in wind power, especially in the Levante area of action (Koletsis et al., 2016), so the literature is inconclusive. On the other hand, there are differences in Poniente annual cycles (Fig. 12) between both periods; specifically, a decrease in its events is observed in the RCP8.5 scenario. In addition, Poniente extension will decrease by 3%–5% by the end of the century, while the number of events will decrease by 5–20 days. Finally, in the study of the time series and their trends, important differences are observed between models regarding their sign and significance (Figs. 11 and 13).

Regional wind dynamics analysis and its comparison between the historical period and the RCP8.5 scenario (Fig. 14, Table 4) shows that all weather regimes, which are similar to those obtained for COSMO-REA6 in Ortega et al. (2023), will not undergo major changes throughout the 21st century. Furthermore, the changes observed are very different between all three models, which may be due to their internal physics. The limitations of these models when studying weather regimes are particularly noteworthy, especially regarding their domain, which does not allow for in-depth study of the Atlantic, and specifically the North Atlantic. Results could be due to small changes in pressure gradient, that are usually sufficient to make the interaction with unique orographic features like the Strait significant (Martín García et al., 1989; García de Pedraza, 1971), but a full synoptic study may be needed to explain what is happening at a dynamic level.

Finally, the extensive scope of calculations has made the selection of limited models and scenarios necessary. First, used CMIP5 models were those that could be obtained with the required resolution at the time of elaboration. In the future, with the arrival of the CMIP6 project, this work should be strengthened with a more robust ensemble. However, CMIP5 models are still useful. A large number of studies have been

conducted on them to examine future changes in wind patterns in the Mediterranean area, especially the interaction between wind and oceanic factors (Islek et al., 2022b,a; Islek and Yuksel, 2022, 2024; Gumuscu et al., 2024). Furthermore, we focused on a single scenario and chose RCP8.5, the most extreme and therefore the one in which the climate change signal is clearest, and also the one for which data are generally most readily available. This has introduced limitations to the work, since the RCP8.5 scenario is not the most likely to occur. These results should be taken as a first approximation for the most extreme signal; further work with the new scenarios proposed by the CMIP6 project should be carried out in the future. Currently, there are some initial wind studies under the equivalent CMIP6 scenario, SSP5-8.5, in the area of interest, although they are still few due to their recent development (Martinez and Iglesias, 2021; Carvalho et al., 2021; Alvarez et al., 2024; Çalışır et al., 2026). These studies project a decline in wind resources for the worst-case scenario throughout the 21st century, which contradicts the general conclusions for CMIP5 scenario and therefore necessitates further research into the physical factors that lead to the differences between the two modelling methods. In any case, the conclusions vary between regions and the methodologies used by each study, making a general evaluation also necessary. We have not found any studies that examine the SSP5-8.5 scenario from the perspective of regional winds in the Iberian Peninsula, which opens up an area for future research.

5. Conclusions

In this work, the ability of a regional climate model ensemble (REMO, MPIOM-REMO, ALADIN63, CNRM-RCSM4 and RegCM4-6) to describe the characteristics of Levante and Poniente winds for present climate conditions (1995–2011) have been studied. Then, the variations that Levante and Poniente may undergo in future projections from different regional climate models have been investigated, comparing the historical period (1950–2005) and the RCP8.5 emissions scenario (2006–2099) of REMO, MPIOM-REMO (24-km) and CNRM-RCSM4 (50-km) models.

Reanalysis-forced RCM results indicate that Levante and Poniente occur around 130–160 days a year in the area. RCMs are able to reproduce the main features described by the reanalysis. In addition, a higher spatial resolution improves the simulation of regional winds. In terms of temporal resolution, the 3-hour data do not introduce errors with respect to the hourly resolution, but the 6-hour data lead to poor reproduction of wind events. Atmosphere-ocean coupling can produce significant differences in wind description compared to uncoupled models, but this varies depending on the studied flow.

Historical and future results show good agreement in wind mean values, distributions and annual cycles with those obtained in the evaluation and with the few references available in the literature. Levante events increase under the RCP8.5 emissions scenario, in some cases in a statistically significant way, up to 10–20 more events per year, i.e. up to 120–140 Levante days per year by the end of the 21st century. On the other hand, both the percentage of Poniente extension and the frequency of its events decrease under the RCP8.5 emissions scenario for all models. Specifically, its extension decreases significantly by 3%–5%, while the number of events will decrease between 5–20 days, also significantly in some cases, resulting in 130–140 Poniente days per year.

Levante influences maritime and coastal activities in the Strait of Gibraltar and the Andalusian coast (García de Pedraza, 1978; Rivera, 2014), so flow alterations could lead to maritime mishaps and require modifications in navigation and transport. Poniente changes could also mean a variation in the rainfall regime on the western Andalusian coast (Tout and Kemp, 1985; Martín García et al., 1989; Viedma Muñoz, 2012). Influence of climate change on Levante and Poniente winds would have consequences for society. This work is expected to serve as an enhancement of further studies focused on regional winds, as they are currently quite scarce, not only for this region but also for others with potential interest. Improving our understanding and characterization of these atmospheric phenomena, with a special focus on the assessment of their climate change signal, can be of high interest.

Although this work was carried out with a limited number of models, those available for the variables of interest with the necessary resolution, future work could extend this ensemble, especially with the new CMIP6 models. Furthermore, although the scope of this article only allowed for the most extreme scenario, RCP8.5, it would be of great interest to compare these results with a more plausible scenario, such as RCP4.5, to determine exactly what the most likely changes are in the areas where these flows occur.

CRediT authorship contribution statement

María Ortega: Writing – review & editing, Writing – original draft, Visualization, Validation, Software, Methodology, Investigation, Formal analysis, Data curation, Conceptualization. **Claudia Gutiérrez:** Writing – review & editing, Visualization, Supervision, Software, Methodology, Investigation, Funding acquisition, Conceptualization. **Noelia López-Franca:** Writing – review & editing, Visualization, Software, Methodology, Investigation, Conceptualization. **María Ofelia Molina:** Writing – review & editing, Visualization, Software, Methodology, Investigation, Conceptualization. **William Cabos:** Writing – review & editing, Resources, Data curation. **Dmitry Sein:** Writing – review & editing, Resources, Data curation. **Enrique Sánchez:** Writing – review & editing, Visualization, Supervision, Software, Resources, Project administration, Methodology, Investigation, Funding acquisition, Conceptualization.

Funding

M. Ortega has been funded through the predoctoral fellowship 2020/3836 by the University of Castilla-La Mancha (UCLM) and the European Social Fund. M. O. Molina was funded by FCT, I.P./MCTES through national funds (PIDDAC): LA/P/0068/2020 - https://doi.org/10.54499/LA/P/0068/2020, UID/PRR2/50019/2025 - https://doi.org/10.54499/UID/PRR/50019/2025. This work has also been funded by the Spanish Ministry of Science and Innovation (MICINN) and the Spanish State Research Agency through national project PID2020-118210RB-C21 (EMERGENTES 100%). This work has been also part of the funded project 2024/00338/001 (REVOLT) of the University of Alcalá. Finally, this work has been partially supported by research project EOLIBER (2025-GRIN-38477) granted by the UCLM Research Plan and co-funded by the European Regional Development Fund (FEDER). This work is also related to SBPLY/24/180225/000026 regional research project, funded by EU-FEDER and JCCM through INNOCAM agency. Open Access funding provided by University of Castilla-La Mancha.

Declaration of competing interest

The authors declare that they have no known competing financial interests or personal relationships that could have appeared to influence the work reported in this paper.

Acknowledgements

We want to acknowledge the Hans-Ertel-Centre for Weather Research Climate Monitoring and Diagnostics (Universities of Bonn and Cologne) and the German Meteorological Service (DWD) for COSMO-REA6 data and documentation, which is available for download (https://reanalysis.meteo.uni-bonn.de/?COSMO-REA6), as well as the Copernicus Climate Change Service (C3S) and its Climate Data Store for ERA5 reanalysis data. We also thank EURO-CORDEX (https://www.euro-cordex.net/060378/index.php.en) and Med-CORDEX (https://www.medcordex.eu/medcordex.php) projects for ALADIN63, RegMC4-6 and CNRM-RCSM4 data and documentation, and the Spanish State Meteorological Agency (AEMET) for its Arcimís repository (https://repositorio.aemet.es/). Finally, we would like to thank Samuel Somot (CNRM) for providing CNRM-RCSM4 pressure data upon personal request.

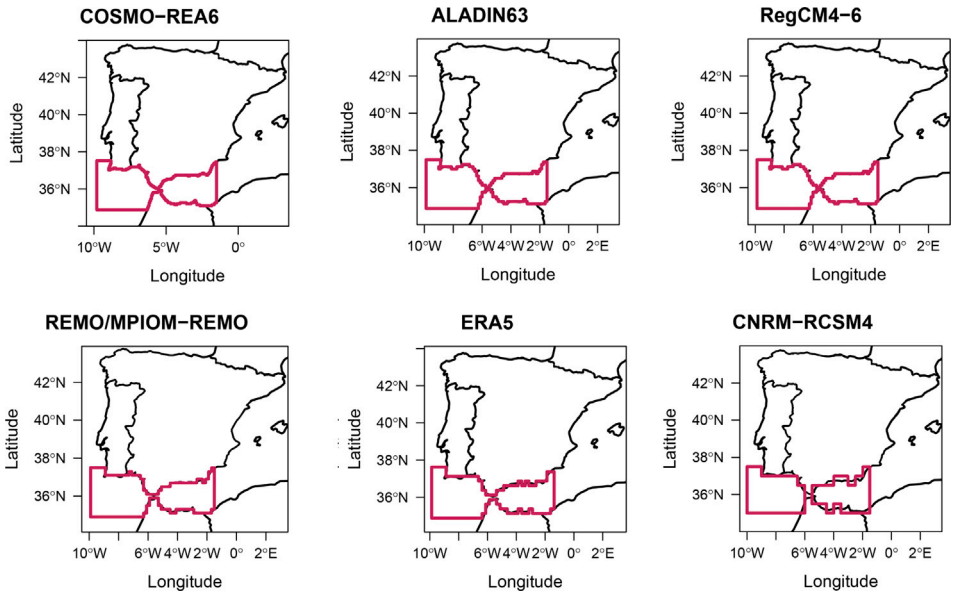

Fig. A.15. Strait of Gibraltar domains for each model. Level of detail depends on the spatial resolution available. Approximate grid spacings are: 31 km (ERA5), 6 km (COSMO-REA6), 24 km (REMO/MPIOM-REMO), 12 km (ALADIN63), 50 km (CNRM-RCSM4) and 12 km (RegCM4-6).

Appendix A. Study domain

The domain used in this work, which differs depending on the model or reanalysis used, can be seen in Fig. A.15.

Appendix B. Temporal resolution influence from ALADIN63 and RegCM4-6 climate models

To quantify whether the differences between temporal resolutions are statistically significant, the Mann–Whitney–Wilcoxon test has been carried out. Results reflect that there are no significant differences when comparing the medians of the wind extension (with p-values of 0.74 in ALADIN63 and 0.88 in RegCM4-6 for Levante; 0.90 in ALADIN63 and 0.88 in RegCM4-6 for Poniente; in any case, all above significance level). That is, the distribution of these characteristics is respected and a lower temporal resolution does not introduce error. If only wind extension were studied, the use of a model ensemble would be feasible. However, wind extension itself does not provide as much information. The hours per day in which Levante and Poniente are detected are always significantly different between both resolutions, with p-values of 0.00 in all cases. That is, the presence of less data makes the calculation of regional wind hours per day and therefore wind events different and generally less accurate at a lower resolution.

For Levante, its distributions (Fig. B.16) are similar to each other. The difference is more notable for Levante hours detected per day. Daily cycles (Fig. B.17) are similar to each other, ALADIN63 always more similar to the reanalysis than RegCM4-6, and they present few differences, although in this case using 6-hourly data overestimates the monthly count of hours.

Finally, Poniente distributions (Fig. B.18) are very similar to those of Levante due to their similar characteristics. The major differences are found in the distribution of Poniente hours per day. In the annual cycles (Fig. B.19), although the monthly averages are respected, 6-hourly data again overestimates the calculation.

Appendix C. Atmosphere-ocean coupling influence from REMO and MPIOM-REMO climate models

A comparison of the REMO/MPIOM-REMO pair with COSMO-REA6 and ERA5 reanalyses can be seen in Fig. C.20, which describes some Levante characteristics. In general, percentage of Levante extension according to REMO/MPIOM-REMO is very similar to ERA5 both in its density and in its annual cycles, but it is not able to detect the summer decrease. These conclusions also apply to the number of hours per day. Results suggest that REMO and MPIOM-REMO are very similar between them and that they are only distinguished because REMO slightly overestimates wind values, especially in winter. These differences have been statistically studied using the Mann–Whitney–Wilcoxon test. For Levante, all characteristics show significant differences when comparing REMO and MPIOM-REMO (p-value of 0.00 for the extension and 0.01 for the number of hours).

For Poniente, the Mann–Whitney–Wilcoxon test does not find significant differences between models, which is visible in their distributions (Fig. C.21), and with p-values of 0.36 and 0.95 for extension and number of hours. This suggests that coupling introduces significant differences in the characteristics of some winds, but not always.

Appendix D. Historical (1950–2005) and future (2006–2099) trends

In the historical period (1950–2005) the trends for Levante extension percentage are significant for all models, but not the number of events (Table D.5). Poniente does not show significant trends in the historical period. Under the RCP8.5 emissions scenario, the percentage of extension shows significant trends for the three models and both Levante and Poniente, while the trend in the number of days is only significant for CNRM-RCSM4.

For 25-year subperiods, none of the trends is significant in the historical simulations (Table D.6). Again, none of the trends for the 25-year subperiods for the RCP8.5 emissions scenario is significant (Table D.7). These results are similar to those found for the evaluation and in Ortega et al. (2023), where study periods are of similar length.

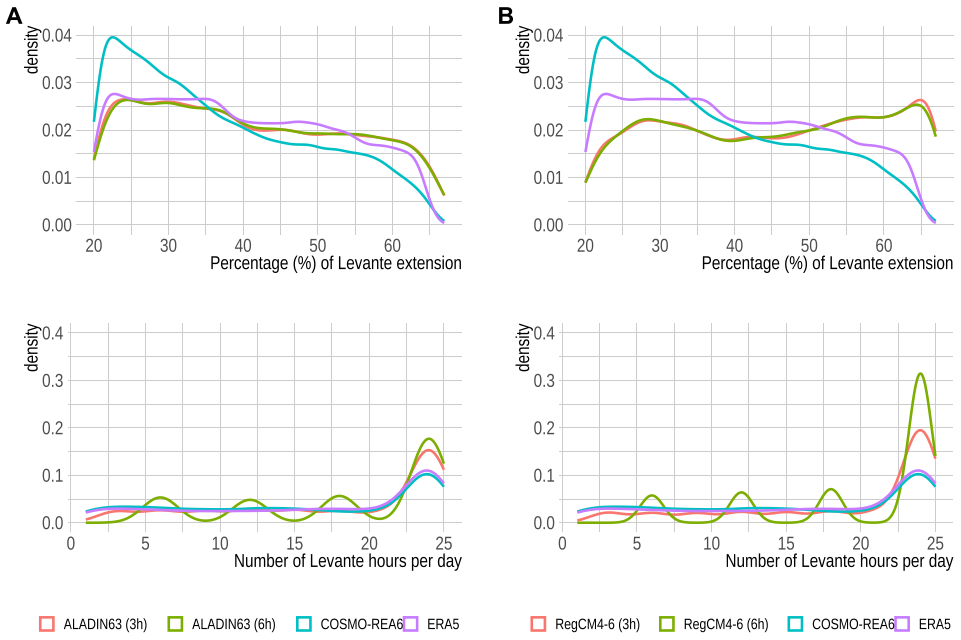

Fig. B.16. Levante extension (top) and number of daily Levante hours (bottom) distributions. A: comparison of ALADIN63 (3 h), ALADIN63 (6 h), COSMO-REA6 and ERA5 in the common evaluation period (1995–2011). B: comparison of RegCM4-6 (3 h), RegCM4-6 (6 h), COSMO-REA6 and ERA5 in the common evaluation period (1995–2011).

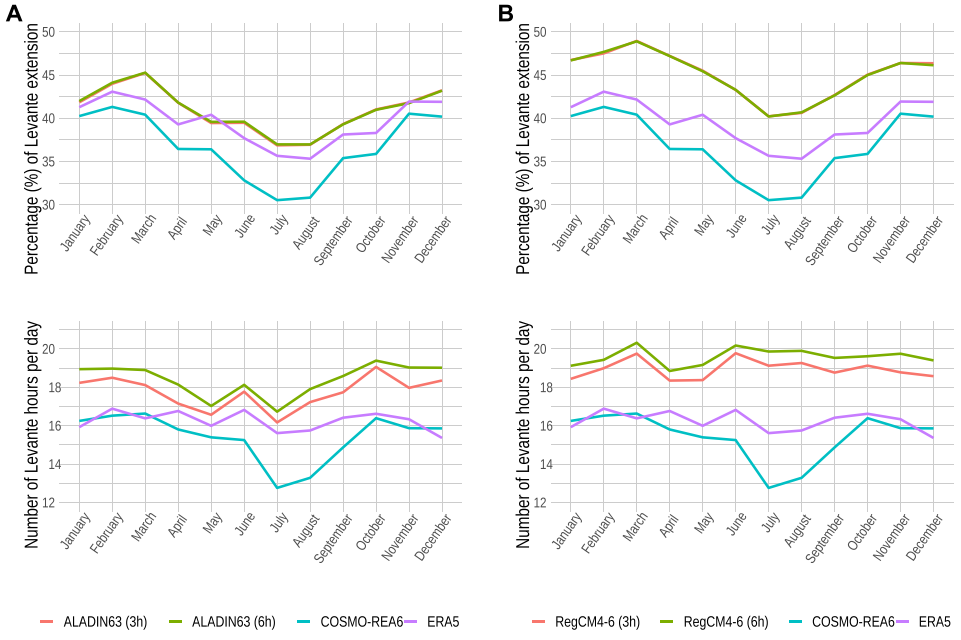

Fig. B.17. Annual cycles from monthly data for Levante extension (top) and number of Levante daily hours (bottom). A: comparison of ALADIN63 (3 h), ALADIN63 (6 h), COSMO-REA6 and ERA5 in the common evaluation period (1995–2011). B: comparison of RegCM4-6 (3 h), RegCM4-6 (6 h), COSMO-REA6 and ERA5 in the common evaluation period (1995–2011).

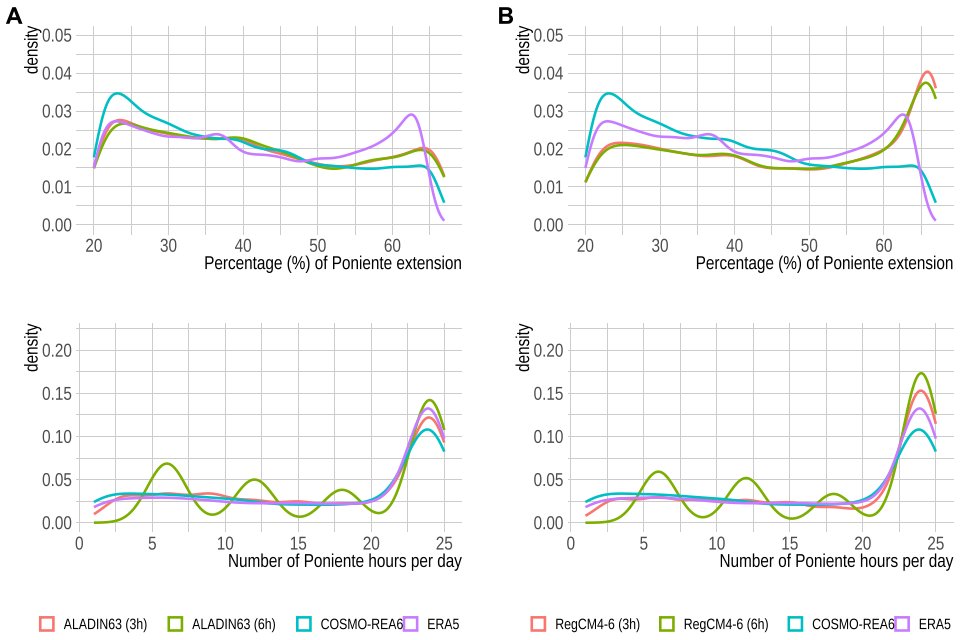

Fig. B.18. Poniente extension (top) and number of daily Poniente hours (bottom) distributions. A: comparison of ALADIN63 (3 h), ALADIN63 (6 h), COSMO-REA6 and ERA5 in the common evaluation period (1995–2011). B: comparison of RegCM4-6 (3 h), RegCM4-6 (6 h), COSMO-REA6 and ERA5 in the common evaluation period (1995–2011).

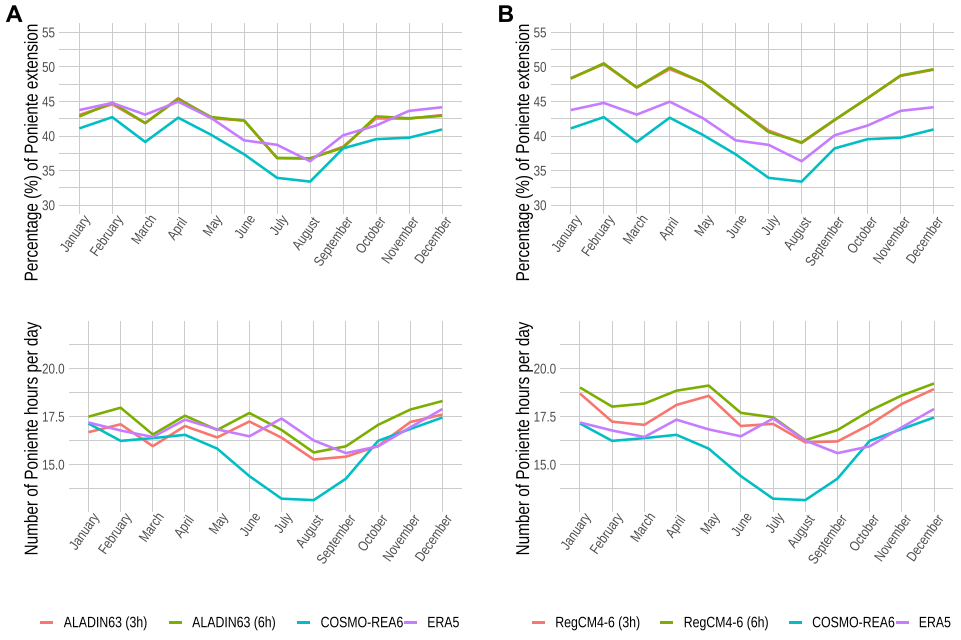

Fig. B.19. Annual cycles from monthly data for Poniente extension (top) and number of Poniente daily hours (bottom). A: comparison of ALADIN63 (3 h), ALADIN63 (6 h), COSMO-REA6 and ERA5 in the common evaluation period (1995–2011). B: comparison of RegCM4-6 (3 h), RegCM4-6 (6 h), COSMO-REA6 and ERA5 in the common evaluation period (1995–2011).

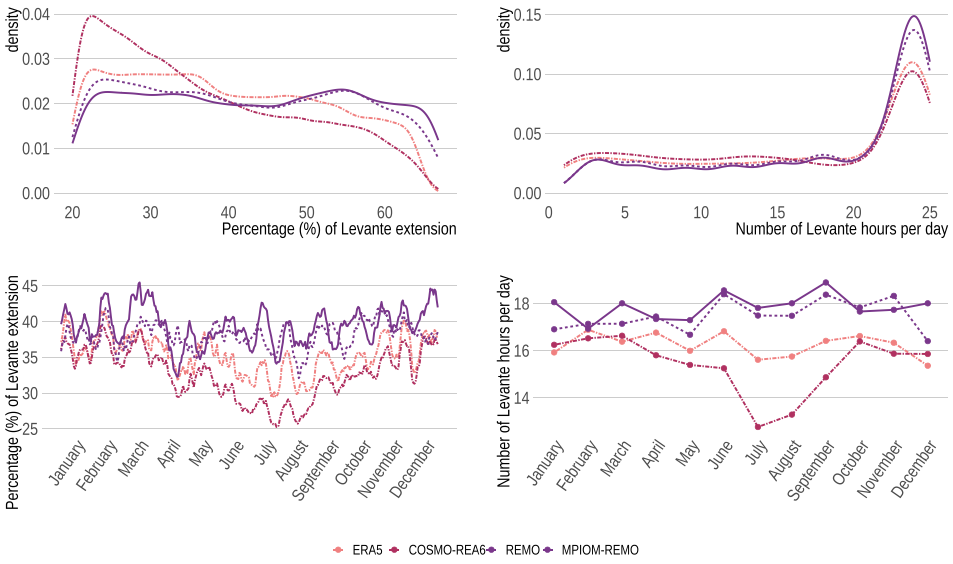

Fig. C.20. Top: distribution of Levante extension and daily Levante hours according to REMO, MPIOM-REMO, COSMO-REA6 and ERA5 over the common evaluation period (1995–2011). Bottom: annual cycles of Levante extension (daily data smoothed with a 10-day moving window) and daily Levante hours (monthly means) according to REMO, MPIOM-REMO, COSMO-REA6 and ERA5 over the common assessment period (1995–2011). Uncoupled models show solid lines; coupled models show dashed lines.

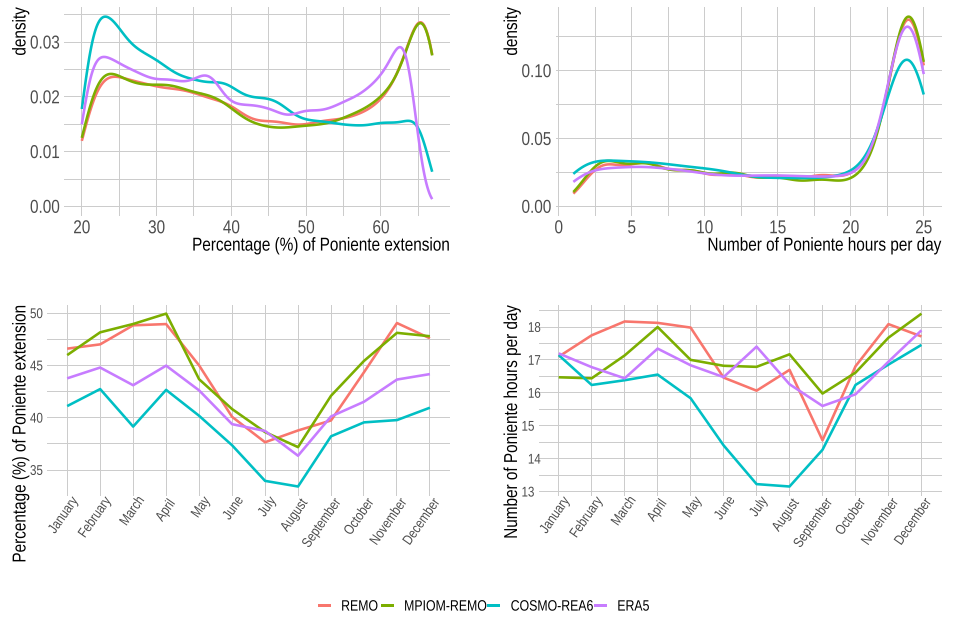

Fig. C.21. Top: Poniente extension and number of Poniente daily hours distributions according to REMO, MPIOM-REMO, COSMO-REA6 and ERA5 over the common evaluation period (1995–2011). Bottom: annual cycles of Poniente extension and number of Poniente daily hours according to REMO, MPIOM-REMO, COSMO-REA6 and ERA5 over the common evaluation period (1995–2011).

Table D.5
Mann–Kendall test coefficients with a significance level $\alpha = 0.05$ for Levante and Poniente extension and number of days per year trends according to various climate models in the historical period (1950–2005) and in the future projection under the RCP8.5 emissions scenario (2006–2099).

HISTORICAL PERIOD (1950–2005)				
	Levante		Poniente	
Model	Extension	Days/Year	Extension	Days/Year
REMO	0.0296	0.7183	0.6644	0.7411
MPIOM-REMO	0.0017	0.4159	0.8432	0.5476
CNRM-RCSM4	0.0321	0.8210	0.4880	0.3883
RCP8.5 EMISSIONS SCENARIO (2006–2099)				
	Levante		Poniente	
Model	Extension	Days/Year	Extension	Days/Year
REMO	0.0000	0.4368	0.0000	0.5133
MPIOM-REMO	0.0000	0.7512	0.0000	0.4406
CNRM-RCSM4	0.0000	0.0005	0.0000	0.0002

Table D.6
Mann–Kendall test coefficients with a significance level $\alpha = 0.05$ for Levante and Poniente number of days per year trends according to various climate models in the historical period (1950–2005), divided into subperiods of approximately 25 years: A (1950–1978) and B (1979–2005).

	Levante		Poniente	
Model	A	B	A	B
REMO	0.2945	0.3422	0.6071	0.5013
MPIOM-REMO	0.4644	0.7816	0.1088	0.7366
CNRM-RCSM4	1.0000	0.3738	0.6211	0.4763

Table D.7
Mann–Kendall test coefficients with a significance level $\alpha = 0.05$ for Levante and Poniente number of days per year trends according to various climate models in the future projections (2006–2099) under the RCP8.5 emissions scenario, divided into subperiods of approximately 25 years: A (2006–2028), B (2029–2053), C (2054–2076) and D (2077–2099).

FIRST HALF OF THE 21st CENTURY				
	Levante		Poniente	
Model	A	B	A	B
REMO	0.2238	0.6739	0.2340	0.7086
MPIOM-REMO	0.6526	0.7082	0.8116	0.7258
CNRM-RCSM4	0.9579	0.0879	0.8533	0.2619
SECOND HALF OF THE 21st CENTURY				
	Levante		Poniente	
Model	C	D	C	D
REMO	0.5434	0.2784	0.8735	0.7910
MPIOM-REMO	0.6340	0.2345	0.8118	0.3689
CNRM-RCSM4	0.9789	0.2556	0.4749	0.1535

Data availability

COSMO-REA6 dataset analysed in the current work is available at opendata-FTP server at the German Meteorological Service (DWD), https://reanalysis.meteo.uni-bonn.de/?COSMO-REA6. ERA5 dataset is available at Copernicus Climate Data Store, https://cds.climate.copernicus.eu/cdsapp#!/dataset/reanalysis-era5-single-levels. ALADIN63 and RegCM4-6 datasets are available at EURO-CORDEX download nodes, https://www.euro-cordex.net/060378/index.php.en. CNRM-RCSM4 dataset is available at Med-CORDEX download nodes, https://www.medcordex.eu/medcordex.php. Finally, REMO and MPIOM-REMO datasets analysed in the current study are available from William Cabos (william.cabos@uah.es) and Dmitry Sein (dmitry.sein@awi.de) on reasonable request.

References

Adloff, F., Jordà, G., Somot, S., Sevault, F., Arsouze, T., Meyssignac, B., Li, L., Planton, S., 2018. Improving sea level simulation in Mediterranean regional climate models. Clim. Dyn. 51, 1167–1178. http://dx.doi.org/10.1007/s00382-017-3842-3.

Ahrens, C.D., Henson, R., 2019. Meteorology Today: An Introduction to Weather, Climate, and Environment. twelfth ed., Cengage Learning, Boston.

Alvarez, I., Pereira, H., Picado, A., Sousa, M.C., Lorenzo, M., Dias, J., 2024. Projection of compound wind and precipitation extreme events in the Iberian Peninsula based on CMIP6. Earth Syst. Environ. 8, 801–814. http://dx.doi.org/10.1007/s41748-024-00429-6.

Anagnostopoulou, C., Zanis, P., Katragkou, E., Tegoulias, I., Tolika, K., 2014. Recent past and future patterns of the Etesian winds based on regional scale climate model simulations. Clim. Dyn. 42 (7), 1819–1836. http://dx.doi.org/10.1007/s00382-013-1936-0.

Belušić Vozila, A., Güttler, I., Ahrens, B., Obermann-Hellhund, A., Prtenjak, M.T., 2019. Wind over the Adriatic region in CORDEX climate change scenarios. J. Geophys. Res.: Atmospheres 124 (1), 110–130. http://dx.doi.org/10.1029/2018JD028552.

Bollmeyer, C., Keller, J.D., Ohlwein, C., Wahl, S., Crewell, S., Friederichs, P., Hense, A., Keune, J., Kneifel, S., Pscheidt, I., Redl, S., Steinke, S., 2015. Towards a high-resolution regional reanalysis for the European CORDEX domain. Q. J. R. Meteorol. Soc. 141 (686), 1–15. http://dx.doi.org/10.1002/qj.2486.

Cabos, W., de la Vara, A., Álvarez-García, F.J., Sánchez, E., Sieck, K., Pérez-Sanz, J.-I., Limareva, N., Sein, D.V., 2020. Impact of ocean-atmosphere coupling on regional climate: the Iberian Peninsula case. Clim. Dyn. 54, 4441–4467. http://dx.doi.org/10.1007/s00382-020-05238-x.

Cabos, W., Sein, D.V., Durán-Quesada, A., Liguori, G., Koldunov, N.V., Martínez-López, B., Alvarez, F., Sieck, K., Limareva, N., Pinto, J.G., 2019. Dynamical downscaling of historical climate over CORDEX Central America domain with a regionally coupled atmosphere–ocean model. Clim. Dyn. 52, 4305–4328. http://dx.doi.org/10.1007/s00382-018-4381-2.

Çalışır, E., Amarouche, K., Çakmak, R., Akpınar, A., 2026. Performance assessment of 22 CMIP6 climate models for projecting wind climate and wind power over the Mediterranean Sea. Environ. Earth Sci. 85, 170. http://dx.doi.org/10.1007/s12665-026-12885-6.

Campins, J., Jansa, A., Benech, B., Koffi, E., Bessemoulin, P., 1995. PYREX observation and model diagnosis of the tramontane wind. Meteorol. Atmos. Phys. 56, 209–228. http://dx.doi.org/10.1007/BF01030138.

Carvalho, D., Rocha, A., Costoya, X., deCastro, M., Gómez-Gesteira, M., 2021. Wind energy resource over Europe under CMIP6 future climate projections: What changes from CMIP5 to CMIP6. Renew. Sustain. Energy Rev. 151, 111594. http://dx.doi.org/10.1016/j.rser.2021.111594.

Casanueva, A., Herrera, S., Fernández, J., Gutiérrez, J.M., 2016. Towards a fair comparison of statistical and dynamical downscaling in the framework of the EURO-CORDEX initiative. Clim. Change 137, 411–426. http://dx.doi.org/10.1007/s10584-016-1683-4.

da Silva, M.L., de Oliveira, C.P., Santos e Silva, C.M., de Oliveira, S.G., Correa, M.J., 2022. Analyzing dynamical downscaling over the Tropical South America using RegCM4. Pure Appl. Geophys. 179, 3859–3874. http://dx.doi.org/10.1007/s00024-022-03153-2.

Dafka, S., Toreti, A., Luterbacher, J., Zanis, P., Tyrlis, E., Xoplaki, E., 2018a. On the ability of RCMs to capture the circulation pattern of Etesians. Clim. Dyn. 51, 1687–1706. http://dx.doi.org/10.1007/s00382-017-3977-2.

Dafka, S., Toreti, A., Luterbacher, J., Zanis, P., Tyrlis, E., Xoplaki, E., 2018b. Simulating extreme etesians over the Aegean and implications for wind energy production in Southeastern Europe. J. Appl. Meteorol. Clim. 57 (5), 1123–1134. http://dx.doi.org/10.1175/JAMC-D-17-0172.1.

de la Vara, A., Cabos, W., Sein, D.V., Claas, T., Jacob, D., 2021. Impact of air–sea coupling on the climate change signal over the Iberian Peninsula. Clim. Dyn. 57, 2325–2349. http://dx.doi.org/10.1007/s00382-021-05812-x.

Denamiel, C., Tojčić, I., Vilibić, I., 2020. Far future climate (2060–2100) of the northern Adriatic air–sea heat transfers associated with extreme bora events. Clim. Dyn. 55, 3043–3066. http://dx.doi.org/10.1007/s00382-020-05435-8.

Denamiel, C., Tojčić, I., Vilibić, I., 2021. Balancing accuracy and efficiency of atmospheric models in the Northern Adriatic during severe bora events. J. Geophys. Res.: Atmospheres 126 (5), e2020JD033516. http://dx.doi.org/10.1029/2020JD033516.

Dunić, N., Supić, N., Sevault, F., Vilibić, I., 2023. The northern Adriatic circulation regimes in the future winter climate. Clim. Dyn. 60, 3471–3484. http://dx.doi.org/10.1007/s00382-022-06516-6.

Elizalde, A., Groeger, M., Mathis, M., Mikolajewicz, U., Bülow, K., Hüttl-Kabus, S., Klein, B., Ganske, A., 2014. MPIOM-REMO: A coupled regional model for the North Sea. KLIWAS Schriftenreihe 17 (58), http://dx.doi.org/10.5675/Kliwas_58/2014_MPIOM-REMO.

Ezber, Y., 2019. Assessment of the changes in the Etesians in the EURO-CORDEX regional model projections. Int. J. Climatol. 39 (3), 1213–1229. http://dx.doi.org/10.1002/joc.5872.

Gaertner, M.A., González-Alemán, J.J., Romera, R., Domínguez, M., Gil, V., Sánchez, E., Gallardo, C., Miglietta, M.M., Walsh, K.J.E., Sein, D.V., Somot, S., Dell'Aquila, A., Teichmann, C., Ahrens, B., Buonomo, E., Colette, A., Bastin, S., van Meijgaard, E., Nikulin, G., 2018. Simulation of medicanes over the Mediterranean Sea in a regional climate model ensemble: impact of ocean–atmosphere coupling and increased resolution. Clim. Dyn. 51, 1041–1057. http://dx.doi.org/10.1007/s00382-016-3456-1.

García-Bustamante, E., González-Rouco, J.F., Jiménez, P.A., Navarro, J., Montávez, J.P., 2008. The influence of the Weibull assumption in monthly wind energy estimation. Wind. Energy 11 (5), 483–502. http://dx.doi.org/10.1002/we.270.

García de Pedraza, L., 1971. Vientos marítimos y terrales en España. In: Agencia Estatal de Meteorología, Servicio Meteorológico Nacional (Ed.), Calendario Meteorofenológico. 1972. Servicio Meteorológico Nacional, Madrid, pp. 161–171, URL http://hdl.handle.net/20.500.11765/552.

García de Pedraza, L., 1978. Algo sobre nuestros vientos. Boletín de la Asociación Meteorológica Española 2 (5), 3–14, URL http://hdl.handle.net/20.500.11765/6965.

García de Pedraza, L., 1990. Características de los vientos en la zona del Estrecho de Gibraltar. In: Agencia Estatal de Meteorología, Instituto Nacional de Meteorología (Ed.), Calendario Meteorológico. 1991. Instituto Nacional de Meteorología, Madrid, pp. 188–201, URL http://hdl.handle.net/20.500.11765/855.

García de Pedraza, L., García Vega, C., 2001. Contrastes climáticos de dos regiones: Cuenca del Ebro frente a Cuenca del Guadalquivir. In: Agencia Estatal de Meteorología, Instituto Nacional de Meteorología (Ed.), Calendario Meteorológico. 2002. Instituto Nacional de Meteorología, Madrid, pp. 231–241, URL http://hdl.handle.net/20.500.11765/1972.

García de Pedraza, L., Reija, A., 1994. Tiempo y clima en España. Meteorología de las Autonomías. Editorial Dossat S.A., Madrid.

Garrido-Perez, J.M., Ordóñez, C., Barriopedro, D., García-Herrera, R., Paredes, D., 2020. Impact of weather regimes on wind power variability in western Europe. Appl. Energy 264, 114731. http://dx.doi.org/10.1016/j.apenergy.2020.114731.

Giorgetta, M.A., Jungclaus, J., Reick, C.H., Legutke, S., Bader, J., Böttinger, M., Brovkin, V., Crueger, T., Esch, M., Fieg, K., Glushak, K., Gayler, V., Haak, H., Hollweg, H.-D., Ilyina, T., Kinne, S., Kornblueh, L., Matei, D., Mauritsen, T., Mikolajewicz, U., Mueller, W., Notz, D., Pithan, F., Raddatz, T., Rast, S., Redler, R., Roeckner, E., Schmidt, H., Schnur, R., Segschneider, J., Six, K.D., Stockhause, M., Timmreck, C., Wegner, J., Widmann, H., Wieners, K.-H., Claussen, M., Marotzke, J., Stevens, B., 2013. Climate and carbon cycle changes from 1850 to 2100 in MPI-ESM simulations for the Coupled Model Intercomparison Project phase 5. J. Adv. Model. Earth Syst. 5 (3), 572–597. http://dx.doi.org/10.1002/jame.20038.

Giorgi, F., 2019. Thirty years of regional climate modeling: Where are we and where are we going next? J. Geophys. Res.: Atmospheres 124 (11), 5696–5723. http://dx.doi.org/10.1029/2018JD030094.

Giorgi, F., Gutowski, W.J., 2015. Regional dynamical downscaling and the CORDEX initiative. Annu. Rev. Environ. Resour. 40 (1), 467–490. http://dx.doi.org/10.1146/annurev-environ-102014-021217.

Gobiet, A., Jacob, D., Euro-Cordex Community, 2012. A new generation of regional climate simulations for Europe: The EURO-CORDEX Initiative. In: EGU General Assembly Conference Abstracts. p. 8211, Provided by the SAO/NASA Astrophysics Data System, URL https://ui.adsabs.harvard.edu/abs/2012EGUGA..14.8211G.

Gómez, G., Cabos, W.D., Liguori, G., Sein, D., Lozano-Galeana, S., Fita, L., Fernández, J., Magariño, M.E., Jiménez-Guerrero, P., Montávez, J.P., Domínguez, M., Romera, R., Gaertner, M.A., 2016. Characterization of the wind speed variability and future change in the Iberian Peninsula and the Balearic Islands. Wind. Energy 19 (7), 1223–1237. http://dx.doi.org/10.1002/we.1893.

Gu, H., Wang, X., 2020. Performance of the RegCM4.6 for high-resolution climate and extreme simulations over Tibetan Plateau. Atmosphere 11 (10), http://dx.doi.org/10.3390/atmos11101104.

Gualdi, S., Somot, S., Li, L., Artale, V., Adani, M., Bellucci, A., Braun, A., Calmanti, S., Carillo, A., Dell'Aquila, A., Déqué, M., Dubois, C., Elizalde, A., Harzallah, A., Jacob, D., L'Hévéder, B., May, W., Oddo, P., Ruti, P., Sanna, A., Sannino, G., Scoccimarro, E., Sevault, F., Navarra, A., 2013. The CIRCE simulations: Regional climate change projections with realistic representation of the Mediterranean Sea. Bull. Am. Meteorol. Soc. 94 (1), 65–81. http://dx.doi.org/10.1175/BAMS-D-11-00136.1.

Gumuscu, I., Sahin, C., Yuksel, Y., Arı Güner, H.A., Islek, F., 2024. Evaluation of future wind climate over the Eastern Mediterranean Sea. Reg. Stud. Mar. Sci. 78, 103780. http://dx.doi.org/10.1016/j.rsma.2024.103780, URL https://www.sciencedirect.com/science/article/pii/S2352485524004134.

Hersbach, H., Bell, B., Berrisford, P., Hirahara, S., Horányi, A., Muñoz-Sabater, J., Nicolas, J., Peubey, C., Radu, R., Schepers, D., Simmons, A., Soci, C., Abdalla, S., Abellan, X., Balsamo, G., Bechtold, P., Biavati, G., Bidlot, J., Bonavita, M., De Chiara, G., Dahlgren, P., Dee, D., Diamantakis, M., Dragani, R., Flemming, J., Forbes, R., Fuentes, M., Geer, A., Haimberger, L., Healy, S., Hogan, R.J., Hólm, E., Janisková, M., Keeley, S., Laloyaux, P., Lopez, P., Lupu, C., Radnoti, G., de Rosnay, P., Rozum, I., Vamborg, F., Villaume, S., Thépaut, J.-N., 2020. The ERA5 global reanalysis. Q. J. R. Meteorol. Soc. 146 (730), 1999–2049. http://dx.doi.org/10.1002/qj.3803.

Hidalgo, P., Gallego, D., 2019. A historical climatology of the easterly winds in the strait of Gibraltar. Atmósfera 32 (3), 181–195. http://dx.doi.org/10.20937/atm.2019.32.03.02.

Islek, F., Yuksel, Y., 2022. Evaluation of future wind power potential and their projected changes in the black sea and possible stable locations for wind farms. Ocean Eng. 266, 112832. http://dx.doi.org/10.1016/j.oceaneng.2022.112832.

Islek, F., Yuksel, Y., 2024. Possible changes and occurrences of future wave power in an enclosed sea using a high-resolution regional climate model. Ocean Eng. 303, 117843. http://dx.doi.org/10.1016/j.oceaneng.2024.117843.

Islek, F., Yuksel, Y., Sahin, C., 2022a. Evaluation of regional climate models and future wave characteristics in an enclosed sea: A case study of the Black Sea. Ocean Eng. 262, 112220. http://dx.doi.org/10.1016/j.oceaneng.2022.112220.

Islek, F., Yuksel, Y., Sahin, C., 2022b. Evaluation of regional climate models and future wind characteristics in the Black Sea. Int. J. Climatol. 42 (3), 1877–1901. http://dx.doi.org/10.1002/joc.7341.

Jacob, D., Elizalde, A., Haensler, A., Hagemann, S., Kumar, P., Podzun, R., Rechid, D., Remedio, A.R., Saeed, F., Sieck, K., Teichmann, C., Wilhelm, C., 2012. Assessing the transferability of the regional climate model REMO to different coordinated regional climate downscaling experiment (CORDEX) regions. Atmosphere 3 (1), 181–199. http://dx.doi.org/10.3390/atmos3010181.

Jacob, D., Teichmann, C., Sobolowski, S., Katragkou, E., Anders, I., Belda, M., Benestad, R., Boberg, F., Buonomo, E., Cardoso, R.M., Casanueva, A., Christensen, O.B., Christensen, J.H., Coppola, E., Cruz, L.D., Davin, E.L., Dobler, A., Domínguez, M., Fealy, R., Fernandez, J., Gaertner, M.A., García-Díez, M., Giorgi, F., Gobiet, A., Goergen, K., Gómez-Navarro, J.J., Alemán, J.J.G., Gutiérrez, C., Gutiérrez, J.M., Güttler, I., Haensler, A., Halenka, T., Jerez, S., Jiménez-Guerrero, P., Jones, R.G., Keuler, K., Kjellström, E., Knist, S., Kotlarski, S., Maraun, D., van Meijgaard, E., Mercogliano, P., Montávez, J.P., Navarra, A., Nikulin, G., de Noblet-Ducoudré, N., Panitz, H.-J., Pfeifer, S., Piazza, M., Pichelli, E., Pietikäinen, J.-P., Prein, A.F., Preuschmann, S., Rechid, D., Rockel, B., Romera, R., Sánchez, E., Sieck, K., Soares, P.M.M., Somot, S., Srnec, L., Sørland, S.L., Termonia, P., Truhetz, H., Vautard, R., Warrach-Sagi, K., Wulfmeyer, V., 2020. Regional climate downscaling over Europe: perspectives from the EURO-CORDEX community. Reg. Environ. Chang. 20, 51. http://dx.doi.org/10.1007/s10113-020-01606-9.

Jerez, S., Trigo, R.M., Vicente-Serrano, S.M., Pozo-Vázquez, D., Lorente-Plazas, R., Lorenzo-Lacruz, J., Santos-Alamillos, F., Montávez, J.P., 2013. The impact of the North Atlantic oscillation on renewable energy resources in Southwestern Europe. J. Appl. Meteorol. Clim. 52 (10), 2204–2225. http://dx.doi.org/10.1175/JAMC-D-12-0257.1.

Josipović, L., Obermann-Hellhund, A., Brisson, E., Ahrens, B., 2018. Bora in regional climate models: Impact of model resolution on simulations of gap wind and wave breaking. Hrvat. meteorološki časopis 53 (53), 31–42, URL https://hrcak.srce.hr/231266.

Jourdier, B., 2020. Evaluation of ERA5, MERRA-2, COSMO-REA6, NEWA and AROME to simulate wind power production over France. Adv. Sci. Res. 17, 63–77. http://dx.doi.org/10.5194/asr-17-63-2020.

Kendall, M.G., 1948. Rank Correlation Methods. Griffin, New York.

Koletsis, I., Kotroni, V., Lagouvardos, K., Soukissian, T., 2016. Assessment of offshore wind speed and power potential over the Mediterranean and the Black Seas under future climate changes. Renew. Sustain. Energy Rev. 60, 234–245. http://dx.doi.org/10.1016/j.rser.2016.01.080.

Kunz, M., Mohr, S., Rauthe, M., Lux, R., Kottmeier, C., 2010. Assessment of extreme wind speeds from Regional Climate Models – Part 1: Estimation of return values and their evaluation. Nat. Hazards Earth Syst. Sci. 10 (4), 907–922. http://dx.doi.org/10.5194/nhess-10-907-2010.

Lorente-Plazas, R., Montávez, J.P., Jimenez, P.A., Jerez, S., Gómez-Navarro, J.J., García-Valero, J.A., Jimenez-Guerrero, P., 2015. Characterization of surface winds over the Iberian Peninsula. Int. J. Climatol. 35 (6), 1007–1026. http://dx.doi.org/10.1002/joc.4034.

Maharana, P., Kumar, D., Dimri, A.P., 2019. Assessment of coupled regional climate model (RegCM4.6–CLM4.5) for Indian summer monsoon. Clim. Dyn. 53, 6543–6558. http://dx.doi.org/10.1007/s00382-019-04947-2.

Mann, H.B., 1945. Nonparametric tests against trend. Econometrica 13 (3), 245–259. http://dx.doi.org/10.2307/1907187.

Mann, H.B., Whitney, D.R., 1947. On a test of whether one of two random variables is stochastically larger than the other. Ann. Math. Stat. 18 (1), 50–60. http://dx.doi.org/10.1214/aoms/1177730491.

Martín García, E., López Muñoz, L., Ávila Rivas, F., 1989. Contribución al estudio y predicción de los vientos en el Estrecho de Gibraltar. In: Agencia Estatal de Meteorología (Ed.), Primer Simposio Nacional de Predictores del INM. Madrid: Instituto Nacional de Meteorología, pp. 49–66, URL http://hdl.handle.net/20.500.11765/3783.

Martinez, A., Iglesias, G., 2021. Wind resource evolution in Europe under different scenarios of climate change characterised by the novel Shared Socioeconomic Pathways. Energy Convers. Manage. 234, 113961. http://dx.doi.org/10.1016/j.enconman.2021.113961.

Mikolajewicz, U., Sein, D.V., Jacob, D., Königk, T., Podzun, R., Semmler, T., 2005. Simulating Arctic sea ice variability with a coupled regional atmosphere ocean sea ice model. Meteorol. Z. 14 (6), 793–800. http://dx.doi.org/10.1127/0941-2948/2005/0083.

Molina, M.O., Gutiérrez, C., Sánchez, E., 2021. Comparison of ERA5 surface wind speed climatologies over Europe with observations from the HadISD dataset. Int. J. Climatol. 41 (10), 4864–4878. http://dx.doi.org/10.1002/joc.7103.

Nabat, P., Somot, S., Cassou, C., Mallet, M., Michou, M., Bouniol, D., Decharme, B., Drugé, T., Roehrig, R., Saint-Martin, D., 2020. Modulation of radiative aerosols effects by atmospheric circulation over the Euro Mediterranean region. Atmospheric Chem. Phys. 20 (14), 8315–8349. http://dx.doi.org/10.5194/acp-20-8315-2020.

Obermann, A., Bastin, S., Belamari, S., Conte, D., Gaertner, M.A., Li, L., Ahrens, B., 2018. Mistral and Tramontane wind speed and wind direction patterns in regional climate simulations. Clim. Dyn. 51 (3), 1059–1076. http://dx.doi.org/10.1007/s00382-016-3053-3.

Obermann-Hellhund, A., Ahrens, B., 2018. Mistral and tramontane simulations with changing resolution of orography. Atmospheric Sci. Lett. 19 (9), e848. http://dx.doi.org/10.1002/asl.848.

Obermann-Hellhund, A., Conte, D., Somot, S., Torma, C.Z., Ahrens, B., 2018. Mistral and Tramontane wind systems in climate simulations from 1950 to 2100. Clim. Dyn. 50 (1), 693–703. http://dx.doi.org/10.1007/s00382-017-3635-8.

Ortega, M., Gutiérrez, C., López-Franca, N., Molina, M.O., Gutiérrez-Fernández, J., Gaertner, M.A., Sánchez, E., 2024. Characterization of summer easterly winds over the inner Iberian Peninsula. Atmos. Res. 304, 107358. http://dx.doi.org/10.1016/j.atmosres.2024.107358.

Ortega, M., Sánchez, E., Gutiérrez, C., Molina, M.O., López-Franca, N., 2023. Regional winds over the Iberian Peninsula (Cierzo, Levante and Poniente) from high-resolution COSMO-REA6 reanalysis. Int. J. Climatol. 43 (2), 1016–1033. http://dx.doi.org/10.1002/joc.7860.

Pal, J.S., Giorgi, F., Bi, X., Elguindi, N., Solmon, F., Gao, X., Rauscher, S.A., Francisco, R., Zakey, A., Winter, J., Ashfaq, M., Syed, F.S., Bell, J.L., Diffenbaugh, N.S., Karmacharya, J., Konaré, A., Martinez, D., da Rocha, R.P., Sloan, L.C., Steiner, A.L., 2007. Regional climate modeling for the developing world: The ICTP RegCM3 and RegCNET. Bull. Am. Meteorol. Soc. 88 (9), 1395–1410. http://dx.doi.org/10.1175/BAMS-88-9-1395.

Radu, R., Déqué, M., Somot, S., 2008. Spectral nudging in a spectral regional climate model. Tellus A: Dyn. Meteorol. Ocean. 60 (5), 898–910. http://dx.doi.org/10.1111/j.1600-0870.2008.00341.x.

Reale, M., Cabos Narvaez, W.D., Cavicchia, L., Conte, D., Coppola, E., Flaounas, E., Giorgi, F., Gualdi, S., Hochman, A., Li, L., Lionello, P., Podrascanin, Z., Salon, S., Sanchez-Gomez, E., Scoccimarro, E., Sein, D.V., Somot, S., 2022. Future projections of Mediterranean cyclone characteristics using the Med-CORDEX ensemble of coupled regional climate system models. Clim. Dyn. 58, 2501–2524. http://dx.doi.org/10.1007/s00382-021-06018-x.

Rivera, A., 2014. Meses y tiempos: Una visión personal de la meteorología de España. Punto Rojo Libros S.L., Sevilla.

Ruti, P.M., Somot, S., Giorgi, F., Dubois, C., Flaounas, E., Obermann, A., Dell'Aquila, A., Pisacane, G., Harzallah, A., Lombardi, E., Ahrens, B., Akhtar, N., Alias, A., Arsouze, T., Aznar, R., Bastin, S., Bartholy, J., Béranger, K., Beuvier, J., Bouffies-Cloché, S., Brauch, J., Cabos, W., Calmanti, S., Calvet, J.-C., Carillo, A., Conte, D., Coppola, E., Djurdjevic, V., Drobinski, P., Elizalde-Arellano, A., Gaertner, M., Galàn, P., Gallardo, C., Gualdi, S., Goncalves, M., Jorba, O., Jordà, G., L'Heveder, B., Lebeaupin-Brossier, C., Li, L., Liguori, G., Lionello, P., Maciàs, D., Nabat, P., Önol, B., Raikovic, B., Ramage, K., Sevault, F., Sannino, G., Struglia, M.V., Sanna, A., Torma, C., Vervatis, V., 2016. Med-CORDEX Initiative for Mediterranean Climate Studies. Bull. Am. Meteorol. Soc. 97 (7), 1187–1208. http://dx.doi.org/10.1175/BAMS-D-14-00176.1.

Sein, D.V., Gröger, M., Cabos, W., Alvarez-Garcia, F.J., Hagemann, S., Pinto, J.G., Izquierdo, A., de la Vara, A., Koldunov, N.V., Dvornikov, A.Y., Limareva, N., Alekseeva, E., Martinez-Lopez, B., Jacob, D., 2020. Regionally coupled atmosphere-ocean-marine biogeochemistry model ROM: 2. Studying the climate change signal in the North Atlantic and Europe. J. Adv. Model. Earth Syst. 12 (8), e2019MS001646. http://dx.doi.org/10.1029/2019MS001646.

Sein, D.V., Mikolajewicz, U., Gröger, M., Fast, I., Cabos, W., Pinto, J.G., Hagemann, S., Semmler, T., Izquierdo, A., Jacob, D., 2015. Regionally coupled atmosphere-ocean-sea ice-marine biogeochemistry model ROM: 1. Description and validation. J. Adv. Model. Earth Syst. 7 (1), 268–304. http://dx.doi.org/10.1002/2014MS000357.

Sevault, F., Somot, S., Alias, A., Dubois, C., Lebeaupin-Brossier, C., Nabat, P., Adloff, F., Déqué, M., Decharme, B., 2014. A fully coupled Mediterranean regional climate system model: design and evaluation of the ocean component for the 1980–2012 period. Tellus A: Dyn. Meteorol. Ocean. 66 (1), 23967. http://dx.doi.org/10.3402/tellusa.v66.23967.

Small, R.J., Carniel, S., Campbell, T., Teixeira, J., Allard, R., 2012. The response of the Ligurian and Tyrrhenian Seas to a summer Mistral event: A coupled atmosphere–ocean approach. Ocean. Model. 48, 30–44. http://dx.doi.org/10.1016/j.ocemod.2012.02.003.

Somot, S., Ruti, P., 2012. The Med-CORDEX initiative: towards fully coupled Regional Climate System Models to study the Mediterranean climate variability, change and impact. In: EGU General Assembly Conference Abstracts. In: EGU General Assembly Conference Abstracts, p. 6080, Provided by the SAO/NASA Astrophysics Data System, URL https://ui.adsabs.harvard.edu/abs/2012EGUGA..14.6080S.

Taylor, K.E., 2001. Summarizing multiple aspects of model performance in a single diagram. J. Geophys. Res.: Atmospheres 106 (D7), 7183–7192. http://dx.doi.org/10.1029/2000JD900719.

Tout, D.G., Kemp, V., 1985. The named winds of Spain. Weather 40 (10), 322–329. http://dx.doi.org/10.1002/j.1477-8696.1985.tb03721.x.

Vautard, R., Kadygrov, N., Iles, C., Boberg, F., Buonomo, E., Bülow, K., Coppola, E., Corre, L., van Meijgaard, E., Nogherotto, R., Sandstad, M., Schwingshackl, C., Somot, S., Aalbers, E., Christensen, O.B., Ciarlo, J.M., Demory, M.-E., Giorgi, F., Jacob, D., Jones, R.G., Keuler, K., Kjellström, E., Lenderink, G., Levavasseur, G., Nikulin, G., Sillmann, J., Solidoro, C., Sørland, S.L., Steger, C., Teichmann, C., Warrach-Sagi, K., Wulfmeyer, V., 2021. Evaluation of the large EURO-CORDEX regional climate model ensemble. J. Geophys. Res.: Atmospheres 126 (17), e2019JD032344. http://dx.doi.org/10.1029/2019JD032344.

Viedma Muñoz, M., 2012. El viento en el litoral de la Península Ibérica y archipiélago balear. Nimbus: Rev. de climatología, Meteorología y paisaje 29–30, 735–751, URL https://dialnet.unirioja.es/servlet/articulo?codigo=4378178.

Voldoire, A., Sanchez-Gomez, E., Salas y Mélia, D., Decharme, B., Cassou, C., Sénési, S., Valcke, S., Beau, I., Alias, A., Chevallier, M., Déqué, M., Deshayes, J., Douville, H., Fernandez, E., Madec, G., Maisonnave, E., Moine, M.-P., Planton, S., Saint-Martin, D., Szopa, S., Tyteca, S., Alkama, R., Belamari, S., Braun, A., Coquart, L., Chauvin, F., 2013. The CNRM-CM5.1 global climate model: description and basic evaluation. Clim. Dyn. 40, 2091–2121. http://dx.doi.org/10.1007/s00382-011-1259-y.

Vrac, M., Yiou, P., 2010. Weather regimes designed for local precipitation modeling: Application to the Mediterranean basin. J. Geophys. Res.: Atmospheres 115 (D12), http://dx.doi.org/10.1029/2009JD012871.

Winterfeldt, J., Geyer, B., Weisse, R., 2011. Using QuikSCAT in the added value assessment of dynamically downscaled wind speed. Int. J. Climatol. 31 (7), 1028–1039. http://dx.doi.org/10.1002/joc.2105.

Xu, X., Huang, A., Huang, Q., Zhang, Y., Wu, Y., Gu, C., Cai, S., Zhu, X., 2022. Impacts of horizontal resolution of the lateral boundary conditions and downscaling method on the performance of RegCM4.6 in simulating the surface climate over Central-Eastern China. Earth Space Sci. 9 (8), e2022EA002433. http://dx.doi.org/10.1029/2022EA002433.